THE EFFECT OF IN-UTERO-THROUGH-POSTNATAL EXPOSURE OF MICE TO PERFLUORINATED COMPOUNDS ON AIRWAY INFLAMMATION AND FUNCTION

BY

MIN HYUNG RYU

A THESIS SUBMITTED TO THE FACULTY OF GRADUATE STUDIES OF

THE UNIVERSITY OF MANITOBA

IN PARTIAL FULFILLMENT OF THE REQUIREMENTS OF THE DEGREE OF

MASTER OF SCIENCE

DEPARTMENT OF PHYSIOLOGY AND PATHOPHYSIOLOGY

THE UNIVERSITY OF MANITOBA

WINNIPEG, MB

ACKNOWLEDGEMENTS

First and foremost, I would like to extend my most sincere gratitude to my parents, who have courageously immigrated to Canada despite the enormous challenges in overcoming financial, language and cultural barriers. Without such courageous acts, I would have never made it this far. I hope this accomplishment make them proud.

My sincere gratitude extends to every individual I have encountered during the course of my study at the University of Manitoba. Through those encounters, I have grown tremendously in the past three years. In particular, I would like to thank my supervisor, Dr. Andrew J. Halayko. He has tirelessly worked to make resources available and led the research team; his effort ensured a strong foundation I could grow and prosper. Dr. Halayko's mentorship was invaluable in shaping me as a scientist, critical thinker, and scholar.

The members of my advisory committee stimulated my growth as a scientist and scholar. Dr. Edwin Kroeger ensured that I considered physiological relevance during my committee meetings, and was always supportive in my academic endeavors. Dr. Richard Keijzer ensured that I considered clinical relevance and challenged me to think beyond science. He has also been a generous mentor and supporter of my career in medicine. Dr. Kent HayGlass, whom I feared at the beginning of my studies because of his candid speech and criticism, made me much stronger and more mature. I thank all three of my committee members for challenging my knowledge and identifying my strengths and weaknesses.

I owe a huge debt of gratitude to all members of the Halayko lab who have accompanied me in this journey of higher education and discovery. In particular, I thank Sujata Basu, Aruni Jha, and Dr. Oluwaseun Ojo. Sujata was the caring ‘mom’ figure in the animal lab and ensured

that I was not only taking good care of animals but also of myself. Her presence always brought a smile on my face – and our love for Apple products bonded us well.

Mr. Aruni Jha - soon to be Dr. Aruni Jha - has been my partner in crime for the past three years in the lab. Aruni, who is a pharmacologist by training, brought the perspective of pharmacological therapeutics into my studies. More importantly, Aruni made sure I went to the gym at least four times a week and often raised controversial topics to discuss in the gym. We discussed topics including but not limited to social justice, religion, reasons for existence and the evilness yet usefulness of wealth.

Dr. Ojo often was in these same conversations and has been a role model for me. His ethic was carefully considered, and his logic was always well thought-out. Beyond the ethics, Sean taught me cell culture, Western blots, qPCR, and ELISA. I utilized the technique he thought me in my weekend projects – bioengineering of human bronchioles for drug testing. Both Sean and Aruni have generously allowed me to take part in their projects and to learn alongside them. Working with them has been truly a transformative experience.

Many others impacted me in the lab and provided generous helping hands. I would like to thank Ms. Karen Detillieux for her generous helping hands with qPCR and writing. Her meticulous coaching on grammar and writing was instrumental in completing this thesis. I would also like to thank Ms. Jacquie Schwartz for helping with histology, Mr. Thomas Mahood for completing qPCR and Mr. Gerald Stelmack for generous assistance and advice throughout my research project. I also remember and thank my colleagues in the lab Andrea Kroeker, Matthew Lytwyn, Pawan Sharma, Soma Tripathi, Vidyanand (Nandu) Anaparti, Behzad Yeganeh, and Saeid Ghavami.

Numerous collaborators supported my project, and I thank them for providing their resources and time. Drs. Mark Loewen and Allan B Becker were the leaders of the NSERC funded PFC project, and the funds to do this research came from their grants. Dr. Charles Wong and Ms. Neda Nikoobakht provided time, money and technical resources to carry out the LC-MS/MS. Dr. John Gordon supported the initial cytokine analysis of bronchoalveolar lavage fluid using enzyme-linked immunosorbent assay. Mr. Hesam Movassagh and Dr. Abdel Soussi Gounni provided support for me to attempt enzyme-linked immunosorbent assay on whole lung lysates. Without their input, this project would be incomplete.

Finally, I thank the funding agencies. Manitoba Institute of Child Health and Manitoba Health Research Council provided a generous stipend and travel support. Deer Lodge Hospital Staff Association, AllerGen-NCE and the University of Manitoba Graduate Student Associations provided generous travel support for me to attend conferences. Natural Sciences and Engineering Research Council of Canada, and the University of Manitoba provided the general funding for the project, research space, and equipment.

CONTRIBUTIONS

Dr. Mark Lowen was the original designer of perfluorinated compound (PFCs) exposure protocol. He prepared PFCs contaminated chow and trained me in pelletizing PFCs contaminated food. Neda Nikoobakht performed LC-MS/MS experiment under Dr. Charles S. Wong's supervision at the University of Winnipeg, Richardson College for the Environment. Thomas Mahood and Karen Detillieux performed and analyzed qPCR.

I dedicate this work to all parents who have had to endure seeing their child gasp helplessly for air during an asthma attack.

TABLE OF CONTENTS

LIST OF TABLES

LIST OF FIGURES

Copyrighted Materials

The work presented in this dissertation was published in a manuscript: **Ryu MH, Jha A, Ojo OO, Mahood TH, Basu S, Detillieux KA, Nikoobakht N, Wong CS, Loewen M, Becker AB, Halayko AJ**. Chronic exposure to perfluorinated compounds: Impact on airway hyperresponsiveness and inflammation. *Am J Physiol - Lung Cell Mol Physiol* 2014; 307(10):L765-774.

American Journal of Physiolology Lung Cellular and Molecular Physiology holds the copyright of the manuscript and the data associated with the manuscript. The journal's policy requires no prior permission to use any of material contained in the manuscript for a use in academic dissertation. However, permission must be obtained for any other purposes.

Figure 5.3, 6.2, 6.4, 6.5, 6.6, 6.8, 6.9 and Table 5.1, 6.1, 6.2, 6.3, 6.4, 6.5, 6.6, 6.7, 6.8,6.9, 6.10, 6.11, 6.12 contain whole or part of data already published in the manuscript. Anyone wishing duplicate the data elsewhere must obtain copyright permission directly from the publisher of *Am J Physiol - Lung Cell Mol Physiol*.

1. ABSTRACT

Perfluorinated compounds, non-degradable xenobiotics in many consumer products, can cause developmental toxicity in experimental animals, and human exposure is associated with asthma symptoms. Here we tested the hypothesis that sustained *chronic* exposure to perfluorooctanoic acid (PFOA), fluorotelomer alcohol (FTOH) and perflurooctanesulfonic acid (PFOS) induces lung dysfunction that exacerbates allergen-induced airway hyperresponsiveness (AHR) and inflammation. Balb/c mice were exposed to ingested PFOA or PFOS (4 mg/kg in chow) from gestation day-2 to 12 weeks by feeding pregnant and nursing dams, and weaned pups. Mice were exposed to inhaled FTOH by housing pregnant, nursing dams and their pups in a cage with one enrichment hut coated with 100 mg of FTOH. Some pups were also sensitized and challenged with ovalbumin (OVA) at 8-9 weeks of age. Serum PFOA was analyzed by liquid chromatograph-tandem mass spectrometry. Lung function was measured using a small animal ventilator. We assayed inflammatory cells in the lung, performed quantitative PCR for lung cytokines, and examined bronchial goblet cell hyperplasia by histology. PFOA ingestion and FTOH inhalation resulted in PFOA accumulation in serum; 4800±1100 ng/mL and 5400±900 ng/mL, respectively. PFOA-alone, but not FTOH- or PFOS-alone, induced a 25-fold increase of lung macrophages. PFOA- or FTOH alone induced AHR. OVA sensitization and challenge in chemical naïve mice induced dramatic accumulation of inflammatory cells in lungs, as well as goblet cell hyperplasia and AHR. PFOA exposure did not affect OVA-induced lung inflammatory cell number but the relative abundance of interferon-γ was 3-fold higher. PFOS exposure *inhibited* OVA-induced lung inflammation, decreasing total cell and macrophages number in lung lavage by 68.7% and 64.8%, respectively. FTOH exposure also inhibited OVA-induced inflammatory cell accumulation. Despite these effects, neither PFOS nor FTOH affected

OVA-induced AHR. In conclusion, here we show that either PFOA or FTOH exposure can induce AHR, but neither one predisposes for exaggerated allergic lung inflammation or AHR. FTOH or PFOS exposure appears to suppress allergic lung inflammation, but does not affect allergic lung dysfunction. Though our data do not reveal PFOA, FTOH or PFOS exposure as a risk factor for more severe allergic asthma-like symptoms, PFOA alone can induce airway inflammation and alter airway function.

2. RATIONALE

Safe for adults, but may be detrimental to the developing fetus

For more than 40 years, the US Food and Drug Administration (FDA) advised "posed no risk for humans" for Bisphenol A (BPA). As a monomer of polycarbonate plastic, BPA had widely been used to make various consumer products such as food storage containers, baby bottles, beverage cans and water pipes. On January 2010, however, the FDA's stance on BPA toxicity was changed to indicate "some concern" for infants and children (1). The FDA's decision to change their stance was based on results from recent studies using novel approaches and different endpoints to show a toxicological impact on the developing brain, mammary glands and the reproductive system (1).

Since the FDA altered their position in 2010, other studies have continued to demonstrate the developmental toxicity of BPA, including the impact on the developing lung and immune system. In particular, two studies in mice and primates revealed that BPA increased susceptibility of acquiring an asthma-like phenotype when exposure occurred during critical phases of lung and immune system development (2,3). Midoro-Horiuti's study showed exposure to BPA spanning both pre- and postnatal periods, but not postnatal exposure alone, augmented allergic airway inflammation and hyperreactivity to suboptimal allergen challenge in mice (2). Likewise, Van Winkle and colleagues demonstrated that BPA disturbed the maturation of conducting airways, especially the secretory cells, during prenatal development and accelerated secretory cell maturation in Rhesus Macaques fetus; therefore exposure to BPA predisposed offspring to lung diseases such as asthma (3). In both instances, these new studies identified a critical window of fetal susceptibility to environmental chemical exposure during lung develop in utero.

The story of BPA strengthens an argument that a "non-toxic" xenobiotic, which has long been thought to pose no risk for humans, can indeed impact developing organs and increase disease susceptibility of exposed people throughout their lifetime. There is a need to assess the impact of other man-made chemicals during critical windows of fetal susceptibility. Here we assessed whether chronic exposure of mice to perfluorinated compounds beginning in utero and continued throughout adolescence can impact susceptibility for development of an asthma-like phenotype.

3. Introduction and Literature Reviews

3.1 Asthma

Asthma is a chronic disease of the airways, characterized by episodic reversible airway narrowing or obstruction that leads to wheezing, chest tightness and shortness of breath. Worldwide, asthma is estimated to affect 300 million people of all ages and ethnic backgrounds (4). In Canada alone, 2.5 million, or 7.2% of the total population, are diagnosed with asthma (5), and the direct annual cost of the disease to the Canadian government is estimated to top $650 million (6). The incident and prevalence of asthma have increased in the past several decades, and the burden of the disease to governments, health care systems, families, and patients is increasing worldwide (7).

Pathological changes commonly observed in a patient with asthma include airway inflammation, airway hyperresponsiveness, and airway structural remodeling. These hallmarks of asthma define the histo-pathological changes that occur in the asthmatic airway. The changes include: inflammatory cell infiltration, airway smooth muscle cell hyperplasia and hypertrophy, mucus hyper-secretion, reticular basement thickening and angiogenesis. Understanding the etiology and characteristics of these markers have provided considerable insight into understanding asthma and have led to relatively effective management of the disease, but not to a cure. Today, management of asthma is directed towards suppressing airway inflammation with inhaled corticosteroids and relieving bronchoconstriction with bronchodilators. Nevertheless, the natural history of asthma still remains unknown, and how modifiable environmental factors may promote the development, increase the severity or limit the resolution of asthma are of great interest.

3.2 Airway inflammation

Airway inflammation is observed in many asthmatic patients and underlies the pathogenesis of allergic asthma. In the current therapeutic approach for asthma, the primary target of therapeutic intervention focuses on airway inflammation and inhaled corticosteroid (ICS) is widely used as a controller medication. In most patients, ICS is effective in controlling the symptoms of asthma and have been shown to significantly improve quality of life for the patient. Nevertheless, there is a sub-group of the asthmatic population that does not response to ICS therapy (8). This reflects the heterogeneous nature of asthma and prompts in-depth investigation of airway inflammation in asthmatics. Here, a brief description of airway inflammation is provided to bring context to the aspect of airway inflammation that is studied in assessing impact of xenobiotic exposure on asthma susceptibility.

Airway inflammation involves both the innate and adaptive arms of the immune system, and the time course of an allergic asthmatic attack occurs over two distinct phases; an early phase and a late phase. Immediate hypersensitivity allergic reactions or the early phase allergic reaction (EAR) are dependent on the degranulation of activated mast cells and peak within 30 minutes of allergen exposure. The early phase involves release of mediators such as histamine, leukotrienes and prostaglandins from mast cells. These mediators act on goblet cells in the airway epithelium to induce mucus secretions, and on airway smooth muscle (ASM) cells to induce bronchoconstriction. Consequently, there is narrowing of the conducting airways and a phasic reduction in the forced expiratory volume in 1 second (FEV_1) during EAR that later returns to normal.

Subsequently to EAR, the late-phase allergic reaction (LAR) evolves and peaks at 6–12 h. It sometime persist for several days. In contrast to the EAR, in which the innate immune

response predominates and edema and vasodilatation mark the histological changes in the lungs, the LAR is characterized by a prominent leukocytic infiltration in the lungs, comprised of eosinophils, T helper (Th) 2 cells and neutrophils. LAR engages components of the adaptive immune system. LAR is initiated by antigen presentation to T-cells, and this results in pro-inflammatory mediator release including eosinophil recruitment. Activated eosinophils and mast cells release granulose proteins such as major basic protein, eotaxin cationic protein including leukotrienes and platelet activating factor that cause further mucus secretions and bronchoconstriction, epithelial cell damage, vascular leakage, and mucosal edema. This late phase results in airway hyperresponsiveness (AHR) and a prolonged reduction in FEV_1 that slowly returns towards normal FEV_1.

By and large, allergic airway inflammation is associated with active T-cell immune response to inhaled antigens. Active T-cell immune responses to inhaled allergens in patients with allergic airway inflammation are biased toward the Th2 phenotype, in contrast to Th1 skewed immunity in normal, healthy individuals. In general, Th1 cells enhance cellular immune responses, while Th2 cells favour humoral antibody production, including IgE, the immunoglobulin associated with allergic conditions. Th1 helper T cells secrete interferon (IFN)-γ, interleukin (IL) -2 and lymphotoxin, which overall suppress Th2 response, while Th2 helper T cells secrete IL-4,-5, and -13. Investigation of the expression of these cytokines in the lung is a measurement of inflammatory status.

The balance between Th1 and Th2 cells is critical in the development of asthma and the imbalance in the T-cell response results in the development of the asthmatic phenotype. For instance, in a murine model of asthma it was demonstrated that deficiency of IFN-γ, a major Th1 cytokine in the lungs, results in prolonged airway eosinophilia and AHR (9). The Th2 derived

cytokines, such as IL-4, IL-5, IlL-9 and IL-13, orchestrate and amplify allergic inflammation in asthma (reviewed in (10)). In particular, IL-13 is both necessary and sufficient to induce eosinophil infiltration in the lungs and cause airway hyperreactivity. Blockage of IL-13 function by an IL-13 neutralizing agent or IL-13 Rα2, reduces allergen-induced asthma phenotypes in mice, and IL-13 deficient mice fail to elicit AHR despite the presence of intact IL- 4 and 5 response in the airway (11,12). In humans, the IL-4/IL-13 signaling pathway attributed to the symptoms experienced by patient with high serum immunoglobulin E (IgE) levels and respectable response to anti-IgE treatment (8).

In essence, the balance between the pro-inflammatory and anti-inflammatory cytokines is pivotal in sustaining a normal airway function. Any immune-modulatory xenobiotic, which alters the intricate balance of Th1 and Th2 cell responses, may promote the development, increase the severity or limit the resolution of allergic inflammation. In this regard, assessment of inflammatory cell recruitment in the lungs, cytokine expression, goblet cell hyperplasia and mucus production are well-established means to evaluate inflammation in the lungs and as such were implemented in this study.

3.3 Airway hyperresponsiveness

Airway hyperresponsiveness (AHR) is a characteristic feature of asthma that describes the state of increased airway sensitivity to an inhaled contractile agonist. It reflects the "twitchiness" or contraction of the airway smooth muscle, causing bronchoconstriction that manifests as an asthma attack. The increased sensitivity of the asthmatic airway is evident primarily in a steeper slope of the agonist dose-response curve and a greater maximal response to a contractile agonist. The physiological implication of airway hyperresponsiveness (AHR) is

two-fold: a *hypersensitive* state such that a smaller concentration of a contractile agonist is required to initiate the bronchoconstriction, and a *hyperreactive* state such that an equal maximum stimulus generates a greater than normal maximal force of contraction and airway narrowing. A hyperresponsive airway exhibits both changes.

Airway responsiveness is measured in both laboratory and clinical settings using inhaled constrictor agonists, such as histamine or methacholine, to challenge the airways and create a dose-response curve. The measurement of AHR is used in the clinics as a diagnostic test to differentiate between healthy and asthmatic patients. For instance, the PC20 test defines a provocative concentration (PC) of methacholine or histamine that causes a 20% decrease in FEV_1. A decrease in PC20 below a clinically defined limit indicates a diagnosis of asthma, and the degree of AHR is associated with the severity of respiratory symptoms and decline in lung function (13).

AHR is composed of at least two semi-independent components: episodic AHR and persistent AHR (14). Episodic AHR is commonly accompanied by airway inflammatory events and is well controlled with first-line anti-inflammatory therapy in most patients. Persistent AHR, conversely, is likely related to structural and physiological changes in the airways and manifest in severe and difficult to treat asthmatics. Its etiology remains to be explored.

To date, several inducers of AHR have been identified. An atopic IgE-mediated allergic response is a well-characterized inducer of AHR. In particular, IL-13 has been shown to be both necessary and sufficient to induce AHR (15). Inhalation of environmental particulates such as ozone and diesel exhaust can also induce AHR through both immune-mediated and non-immune-mediated pathways (16,17). Therefore, environmental pollutants, especially those that persist in the environment, pose a public health concern because they may increase the

susceptibility for developing AHR. In particular, early life exposure to both immune and non-immune mediated disturbances may impact the normal lung development and impact lung health throughout life.

3.4 Early life asthma development

Asthma affects people of all ages, but most often it starts during childhood. Genetics undoubtedly play a role in asthma development. For instance, polymorphism in the disintegrin and metalloprotease 33 (ADAM33) gene is associated with reduced lung function in infants and development of bronchial hyperresponsiveness (BHR) later in life (18). Environmental factors also influence the disease development, and exposure to microorganisms, pollutants, allergens, and diet can impact one's tendency to develop the disease phenotype.

Epidemiological studies have correlated increased exposure to airborne pollutants during pregnancy with increased susceptibility to childhood asthma (19). Cigarette smoking during pregnancy is linked to a greater incidence of physician-diagnosed asthma (20), and maternal infection during pregnancy is a risk factor for asthma in the offspring (21). Experimentally, a maternal allergic immune response during pregnancy promotes allergy development in the offspring; mouse's pups that were born from allergen sensitized and challenged dams have an increased susceptibility to develop more severe asthma phenotypes (22). Likewise, maternal exposure to particulate matters during pregnancy augments postnatal ozone-induced airway hyperreactivity in juvenile mice (23). Notably, pulmonary exposures to both allergic (i.e. diesel extract particles) and immunologically "inert" (i.e. TiO2) particles during pregnancy caused increased neonatal asthma susceptibility (24). It follows that both an allergic response in the pregnant mother and physiological and environmental insults *in utero* impact the asthma

susceptibility of the offspring.

3.5 Exposure to perfluorinated compounds

Perfluorinated compounds (PFCs) are man-made chemicals used in a variety of industrial and consumer products, including protective coatings for carpets and apparel, consumer housewares, food packaging, and electronics. Their unique polyfluorinated structure and polarity provide extreme resistance to degradation and thus makes PFCs very useful as stain repellents. Despite their usefulness in manufacturing of consumer products, the chemicals' extreme persistence poses a concern to the environment and human health because PFCs are being detected in a variety of environment matrices such as air (25-27), drinking water (28), sediment (29), and house dust (25,26) and accumulate in biological systems (29).

PFCs accumulate in the human body, particularly in the serum, and are detected in both blood (30,31) and breast milk (32). PFCs tend to have a long biological half-life; perfluorooctanoic acid (PFOA) and perfluorooctane sulfonate (PFOS), the two most predominant forms of PFCs found in the environment and human blood, have a human elimination half-life of 3.8 years and 5.4 years, respectively (33). More importantly, PFC exposures are not limited to occupational workers, and exposure is a worldwide phenomenon. PFCs have been found in serum and plasma collected from the general population in Asia (34), Australia (35), Europe (36), North America (31), and South America (36). Serum PFOA and PFOS levels in the general public are in the low nanograms per milliliter range, but PFOA concentrations have been detected at levels up to 478 ng/mL in non-occupational persons (37). Workers occupationally exposed to PFOA and PFOS have serum levels of these chemicals approximately one order of magnitude higher than those reported in the general population (see review (38)). For instance, PFOA serum concentrations reported in occupational workers were

between 422 and 999 ng/mL, and between 155 and 556 ng/mL for individuals living in an area of high environmental exposures (37). In a separate study, serum PFOA concentration measured in retired fluorochemical production workers ranged from 72 ng/mL to 5100 ng/mL, with an arithmetic mean value of 691 ng/mL in 26 exposed individuals (33).

The routes of exposure to PFCs are diverse and include exposure through diet, water intake, air inhalation, dust ingestion and absorption through direct skin contact with consumer products (25). Ingestion is believed to be a key exposure route given a high abundance of PFCs in our diet and food packaging; Canadians, for instance, are estimated to have exposure of ~250 ng/day through diet (39). Another significant means of exposure is inhalation. Fluorotelomer alcohol (FTOH), one of the volatile forms of PFCs and a precursor to PFOA, is detected in the North American troposphere at concentrations up to 165 pg/m^3(27) and in Canadian indoor air at the concentration up to 2900 pg/m^3 (25). Given that we take approximately 22 000 breaths a day or 8 million breaths a year, the accumulated exposure ought to be significant. In addition to the two major exposure routes, small children and toddlers touch, ingest and inhale house dust. Toddlers ingest about 60 mg of house dust per day in modern homes. This translates to about 25 ng of PFCs/day exposure in toddlers (25). This amount is significantly greater than adults who ingest less than 1 ng/ day from dust (25).

3.7 PFOA and PFOS exposure and health outcome

To date, the findings of epidemiological and medical surveillance studies are mixed with no consistent association between serum PFC level and adverse health effects (reviewed in (38,40)). Earlier epidemiological studies found no strong association between serum PFC concentrations and health outcomes: mortality, cancer incidence, potential endocrine effects,

hematology, hormonal and clinical chemistry parameters (37,41-43). One occupational cohort study found an association between the serum concentration of PFOS with increased bladder cancer occurrence (43). However, the bladder study lacked a sufficient sample size, and a larger study on separate cohorts later failed to establish the same association (42,43). Perhaps the accumulated PFOS level was linked to bladder cancer because bladder cancer itself limited renal excretion of PFCs.

In contrast, more recent large studies point to developmental exposure of PFCs as more relevant and serious in its impact on individual health, through delayed development and increased susceptibility to chorionic diseases. For instance, a Danish study in 2007 found a significant negative correlation between maternal plasma PFOA and birth weight (44). A more recent Taiwanese study involving ~450 children revealed that PFC exposure was associated with juvenile asthma; investigators found a positive association between the serum PFC concentration and at least two of the three immunological biomarkers (Serum IgE, absolute eosinophil count and eosinophilic cationic protein level) in asthmatic children (45). Anderson-Mahoney found that people who had been exposed to PFOA via drinking water showed evidence of higher self-reported shortness of breath and asthma (46).

PFOA and PFOS cross the placental barrier and therefore exposure begins *in utero* and spans all critical stages of development in human (47). PFCs have shown the potential for genotoxicity and developmental toxicity *in vitro* and *in vivo* (42,48). Additional studies are needed to further characterize the impact on specific target organs and to elucidate the long-term consequences of prenatal exposures.

3.8 Developmental exposure of PFCs

In both rat and mouse, exposure to PFOS and PFOA during *in utero* development compromised the newborns survival and impeded postnatal growth and development of the survivors (49-52). Moreover, the development toxicity was shown in a dose-dependent manner and high doses (>10mg/kg) caused 100% the neonatal mortality (49-52). Interestingly, the neonatal mortality in rat did not require PFOS exposure before day 19 of gestation, implying that mortality is a result of insufficient development in the late gestational period (51). Similarly, the critical window of PFOA exposure in mice for neonatal mortality is gestation day (GD) 15-17 (50). These observations suggest that organ systems that develop late in gestation may be the targets for PFOS and PFOA insults.

Indeed, PFOS and PFOA was suggested to inhibit or delay perinatal lung development by Grasty et al. (2003, 2005) because of the significant histological and morphometric differences between control and PFOS-exposed lungs of newborns (51,52). Grasty and colleagues found thicker alveolar walls in the lungs of PFOS-exposed mice compared to the controls, and the ratio of solid tissue to small airway was increased, suggesting immaturity. Other investigators indeed observed respiratory insufficiency that caused premature death in newborns pups born from PFOA and PFOS-exposed dams (49). The surviving pups in the developmental toxicology tests significantly lagged behind in body weights compared to those who were not exposed to PFOA or PFOS.

All these data suggests that an exposure during critical stages in pregnancy can induce permanent organ damage, resulting in increased disease susceptibility in the offspring. Compromised immune and lung development may impair the normal recovery process from everyday insults to the lungs. Therefore, the consequences that *in-utero* through postnatal

exposure to PFOA and PFOS has on overall pulmonary function need to be evaluated. In considering suitable animal models, the longer elimination half-lives in mice (17-19 days) relative to other experimental animals such as rat (2hrs - 6 days with gender variance), rabbit (5-7 hrs) and chicken (4.6 days), makes mice the most suitable for use in a low dose chronic exposure model (40).

3.9 PFOA, PFOS and pulmonary surfactant

The intricate regulation of surface tension at the air-liquid interface in alveoli permits us to breathe with ease. Pulmonary surfactant plays a vital role in maintaining low surface tension so that alveoli are prevented from collapsing. Disturbances in pulmonary surfactant function may be detrimental in overall lung function and can have life threatening consequences. For example, babies born with congenital surfactant deficiency will die from respiratory distress shortly after birth unless treated with synthetic surfactant. Therefore, any xenobiotics that interfere with surfactant function can ultimately have a profound impact on the overall respiratory function.

Perfluorinated compounds are widely used as industrial surfactants and have the potential to disturb normal pulmonary surfactant function. Several investigators have examined the interaction of PFCs with pulmonary surfactants. For instance, Lehmler *et al.* (2006) examined the mixing behavior of PFOS with dipalmitoyl phosphatidylcholine (DPPC), a major component of pulmonary surfactant. They observed the behavior by utilizing differential scanning calorimetry and fluorescence anisotropy measurements. Both PFOS and PFOA had a high tendency to partition into lipid bilayers (53). In fact, surfactant surface tension measured using a captive bubble surfactometer demonstrated both PFOA and PFOS were capable of interfering

directly with surfactant properties *in vitro* even at relatively low concentrations (54).

However, *in vivo* assessment of the concentration and molecular speciation of phospholipids, as an indicator of pulmonary surfactant abnormalities and lung maturity revealed no impact of PFC exposure on either of the two parameters (51,52). Furthermore, an attempt to rescue PFOS-induced respiratory failure of newborn rats with agents that are known to promote lung maturation and pulmonary function such as dexamethasone or retinyl palmitate did not succeed. It was, therefore, concluded that the "labored breathing and subsequent mortality observed in the PFOS-exposed newborns might not be related to surfactant deficiency or immaturity of the lung per se" (51).

3.10 PFOA and PFOS modulate immune function by acting as a agonist for PPAR

Although previously thought to be inert, both PFOA and PFOS are now known agonists for peroxisome proliferator-activated receptors (PPAR) α, β and γ (55). PPARs are widely expressed in diverse cell types including immune cells and pulmonary structural cells and act as a regulator of gene transcription through binding to specific response elements or peroxisome proliferator response elements (PPREs). PPARγ, in particular, regulates apoptosis, cell differentiation, energy metabolism, and inflammation (56). PPARγ activation prompts anti-inflammatory effects demonstrated by the inhibition of pro-inflammatory cytokine (TNF-α, IL-1β, IL-6) production by a PPARγ agonist (57). Activated PPARγ stimulates the differentiation of monocytes to macrophages, inhibits the induction of inducible nitric oxide synthase, metallanoproteinase-9 and scavenger receptor A transcription (58). PPARγ activation inhibits the expression of monocyte chemoattractant protein-1, vascular cell adhesion molecule-1, and intracellular adhesion molecule; thus PPARγ activation hinders with chemo-attraction and cell

adhesion of monocytes and T-lymphocytes (57). PPARγ also acts as a trans-repressor of macrophage inflammatory genes (59). Indeed, PFOA has been shown to augment calcitriol-induced monocytic differentiation of the HL-60 (macrophage) cell line, and interestingly, both PPARα and γ agonist administration inhibit allergen-induced airway inflammation in mice, and have been proposed to have possible therapeutic use in asthma (60).

PFOA and PFOS show greater affinity for and activation of PPARα than PPARγ, suggesting that the main target for both PFCs is PPARα (55). PPARα agonists, such as gemfibrozil, ciprofibrate, and fenofibrate have been demonstrated to indirectly increase the production of IL4 and inhibit interferon-gamma (IFNγ) to shift the cytokine balance (61). Moreover, PFOA has been shown to modulate human mast cells *ex vivo* to secrete more pro-inflammatory cytokines such as tumor necrosis factor (TNF)-α, which can directly modulate airways to become hyperresponsive (62). Therefore, PFC activation of PPARs is likely to have a diverse impact on lung immune response. Evaluation of the overall net impact on the local inflammatory response is of great interest and is necessary to gauge a potential link between *in-utero*-through-postnatal exposure to PFCs and asthma susceptibility.

4. HYPOTHESIS AND OBJECTIVES

Hypothesis: Sustained *chronic* exposure of mice to perfluorooctanoic acid (PFOA), fluorotelomer alcohol (FTOH) or perfluorooctanesulfonic acid (PFOS) induces lung dysfunction that exacerbates allergen-induced airway hyperresponsiveness (AHR) and inflammation.

Specific objectives:

1. Assess the impact of chronic PFC exposure on body and liver weight
2. Measure accumulated serum concentration of PFOA in mice that ingested PFOA or inhaled FTOH
3. Determine if PFC exposure in the absence of allergen challenge will result in changes in respiratory mechanics
4. Assess leukocyte accumulation, cytokine mRNA abundance and goblet cell hyperplasia in lungs of pups who were exposed to PFOA, FTOH or PFOS
5. Determine if PFC exposure changes the magnitude of ovalbumin (OVA) induced AHR
6. Determine if PFC exposure will impact OVA induced leukocyte infiltration and goblet cell hyperplasia of the lung

5. MATERIALS AND METHODS

Methods were previously described in a manuscript published by our group (Ryu et al. 2014) and are described here with more details (63).

5.1 Chemicals and reagents

Perfluoro-*n*-octanoic acid (PFOA) (purity > 98%), and the corresponding isotropically labeled standard perfluoro-*n*-[1,2,3,4-$^{13}C_4$]octanoic acid (PFOA-$^{13}C_4$) (purity ≥ 99% ^{13}C) were purchased from Wellington Laboratories (Guelph, ON, Canada). Heptadecafluorooctanesulfonic acid potassium salt (PFOS, ≥98%) was purchased from Sigma-Aldrich (St. Louis, MO, U.S.A.). 2-Perfluorooctylethanol (8:2 FTOH, ≥98%) was purchased from Wellington Laboratories.

5.2 Animals

Balb/c mice were purchased from University of Manitoba Central Animal Care Services (U of M CACS) and were housed in a controlled pathogen free environment (12 hours dark/light cycle). Mice were fed with in-lab pelletized LabDiet 5001 Rodent powder diet (Brentwood, MO, USA). Females were timed mated, and the appearance of a vaginal plug was designated as a gestation day (GD) 0. All animal procedures were performed according to standard operating procedures and guidelines approved by the Animal Ethics Committee, University of Manitoba.

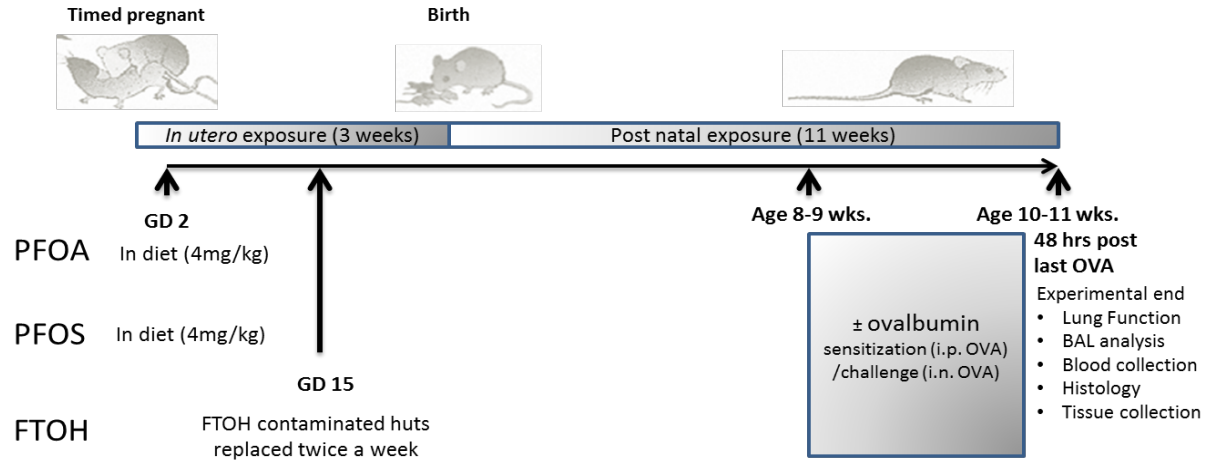

Fig 5.1. *Schematic timeline summary of PFCs exposure protocol.* For dietary exposure, time-mated Balb/c female dams were fed PFOA or PFOS contaminated diet (4 mg chemical/kg diet) beginning gestation day (GD) 2 and throughout pregnancy and lactation period. Pups continued on the same diet after weaning. For inhalation exposure, dams were housed with a FTOH contaminated mouse hut coated with 100 mg of 8:2 FTOH starting GD 15. FTOH exposed pups were kept in the same environment during and after weaning. At age 8-9 weeks, some pups from each exposure cohort were sensitized twice (2 µg OVA/2 mg alum in saline injection i.p.) and challenged three times (50 µg OVA in 50 µl saline applied i.n.) with ovalbumin (OVA). At 48 hrs post final OVA challenge, or 10-11 weeks of age, offspring were assessed for lung function and were sacrificed to collect bronchoalveolar lavage fluid, blood, lung and liver.

5.3 Chemical Exposure

Dietary PFOA and PFOS exposure: Timed-pregnant dams were fed PFOA or PFOS contaminated diet *ad libitum* (~ 4-6 g/day) beginning GD 2. The chemical contaminated diet was prepared by mixing in 4 mg of PFOA or PFOS (dissolved in methanol) per 1 kg of LabDiet 5001 Rodent powder diet (Brentwood, MO, USA). Powder diet was pelletized and dried for three days in a fume hood. Pellets were stored at -20 °C until feeding. The pregnant dams were fed the contaminated diet throughout pregnancy and lactation. The offspring were continued on the same diet after weaning and were then sacrificed at 10-11 weeks of age.

Inhaled FTOH exposure: 8:2 FTOH exposures was carried out by housing the pregnant dam with FTOH contaminated mouse enrichment huts starting GD 15. Enrichment huts were 11 cm length x 11 cm width x 5 cm height (shown in fig 5.2) and were sprayed with 2 mL of 50mg/mL 8:2 FTOH dissolved in methanol. Mice were housed in a cage (43cm length x 23 cm width x 22

cm height) with one contaminated enrichment hut, which was replaced twice a week. The pups remained in this environment during and after weaning.

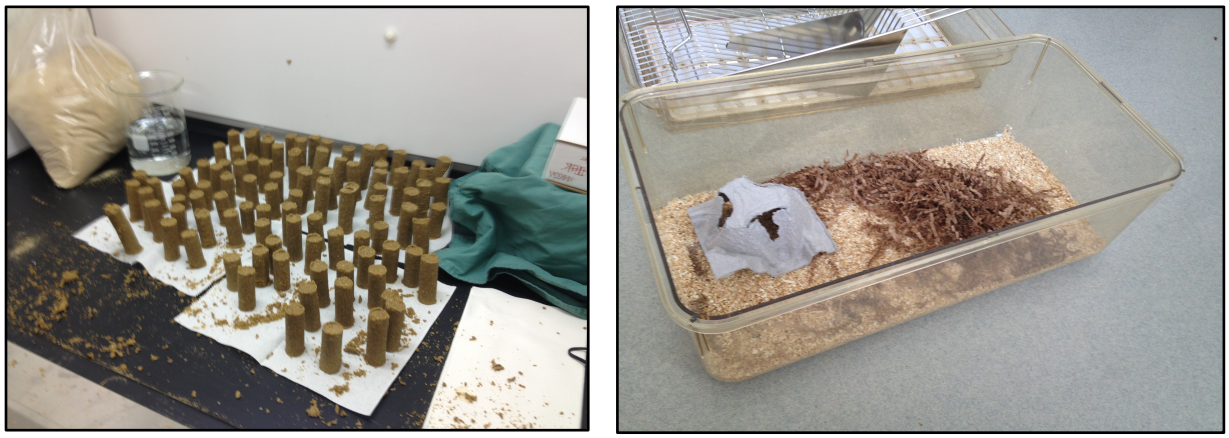

Fig 5.2. *Preparation of dietary PFOA and PFOS pellets and FTOH contaminated huts.* **(LEFT)** In-lab pelletized contaminated diet was prepared by mixing in 4 mg of PFOA or PFOS per 1 kg of LabDiet 5001 Rodent powder diet. Each pellet was cylindrical in shape with dimension of 2.5 cm diameter and 9 cm height. Pellets were dried under chemical safety hood for three days and stored at -20 °C until feeding. **(RIGHT)** Holding cage (43cm length x 23 cm width x 22 cm height) with one FTOH contaminated enrichment hut (11 cm length x 11 cm width x 5 cm height). During the FTOH exposure protocol, huts were changed twice a week.

5.4 LC-MS/MS analysis of PFOA level in serum

Blood collection and sample extraction

At the experimental endpoint, whole blood was collected, left at room temperature to clot and centrifuged at 10000 rpm for 10 min at 4 °C. The supernatant was isolated and stored at -80 °C until extraction and analysis. The PFOA extraction procedure was adopted from a recent study. Briefly, 20 µL of 2.5 pg/µL internal standard mixture, 50 µL of methanol and 50 µL of serum were mixed. The solutions were vortex-mixed, then centrifuged at 14,000 rpm for 10 min. The supernatant was isolated, vortex-mixed with 60 µL of acetonitrile and chilled at -20^{o}C for 1 hour. The mixture was centrifuged at 14,000 rpm for 10 min. 110 µL of supernatant was combined with 110 µL of 0.1% formic acid in a polypropylene auto-sampler vial. The solution was vortexed and then subjected to liquid chromatography mass spectrometry (LC-MS/MS) analysis using online solid phase extraction (SPE) as described previously by McConkey (86). In

brief, the mobile phase gradient from the quaternary pump started at 5% methanol and 95% formic acid (0.1% in water), then increased to 50% methanol and 50% acetonitrile after 90 s, was held 3 min then 100% (50:50) isopropyl alcohol:water for 4 min and finally changed to 50:50 acetonitrile:methanol for 1 min. The binary pump mobile phase gradient for analytical separation was initially 2mM ammonium acetate in water and held for 90 s, then changed to (60:40) acetonitrile:2 mM ammonium acetate during 3 min, held on for 30 s, increased to (67:33) acetonitrile:2 mM ammonium acetate in 36 s , finally raised to 90:10 (2mM acetonitrile:ammonium acetate) and was held for 2 min, decreased to (15:85) acetonitrile: 2mM ammonium acetate in 1 min held for 1 min.

The mass spectrometry analysis was performed using dynamic multiple reaction monitoring using electrospray ionization in negative mode. The curtain gas temperature was set to 300 ^{o}C at a flow of 10 L per minute. The nebulizer pressure was set to 55 psi and the capillary voltage was -2000 V. The LC-MS-MS acquisition was performed in multiple reactions monitoring (MRM) mode by following the transitions *m/z* 413→368.9, *m/z* 413→168.9 and m/z 417→371.9 for the quantifier, qualifier, and the internal standard respectively. Optimized fragmentor voltage 72V and collision energies 16 and 4 V (for qualifier and quantifier respectively) were applied in the method.

LC-MS/MS Quality assurance

PFOA was quantified by isotope dilution. The limit of detection and limit of quantification in bovine plasma were determined as the concentrations with signal-to-noise ratios of three and ten respectively, and were estimated to be 0.014 and 0.048 ng/mL respectively. Percent recoveries of PFOA were determined to be 103%. These results are similar to what has been seen for recoveries in other studies (31,63,64,65).

5.5 Ovalbumin Allergen Challenge

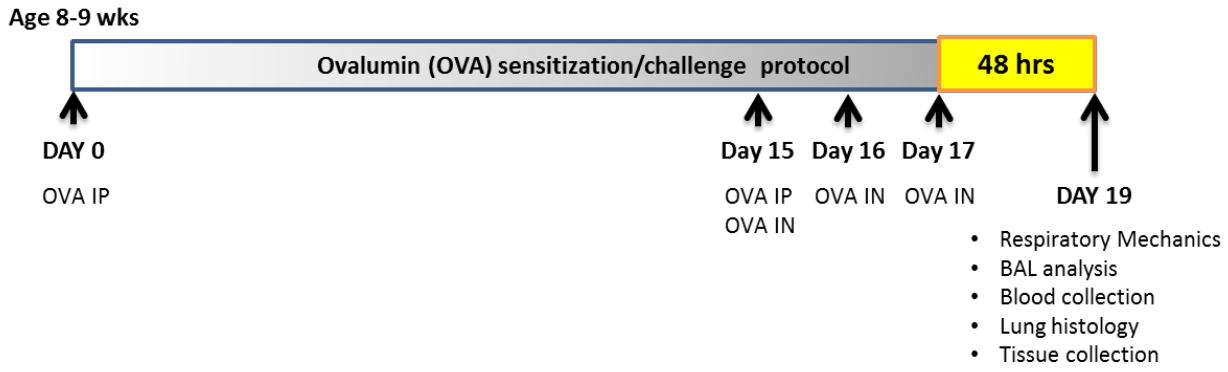

Fig 5.3. *Schematic summary of ovalbumin (OVA) protocol and experimental endpoint*. At age 8-9 weeks, randomly selected pups from each exposure cohort were sensitized to OVA on day 0 and 15 of OVA protocol, by intra-peritoneal injection of 0.5mL saline with 2 µg OVA adsorbed to 2 mg alum. On day 15, 16, and 17, mice were challenged intra-nasally (i.n.) with 50 µg OVA in 50 µl saline. At 48 hrs post final OVA challenge, offspring were assessed for respiratory mechanics. Lungs were lavaged after the lung mechanics, and total number of cells in bronchoalveolar lavage was estimated. Blood and tissues were collected after the lung function measure. For histology, lungs were inflated and fixed with 1mL of 10% buffered formalin (pH 7.4) to a pressure of 25 cm H_2O.

To assess the effect of PFC exposure on the allergen induced airway inflammation and airway hyperresponsiveness (AHR), we subjected some mice from the chemical exposed cohorts to ovalbumin (OVA) sensitization and challenge. On day 0 of OVA protocol (8-9 weeks of age), mice were sensitized by intra-peritoneal (i.p.) injection of 2 µg of OVA (Albumin Chickeng Egg Grade V, Sigma-Aldrich) adsorbed to 2 mg alum (Inject® Alum, Thermo Scientific) in 0.5mL saline. 15 days after the first OVA sensitization, a second dose of i.p. OVA was administered. Concurrent to the second i.p. OVA, mice were challenged with intra nasal (i.n) OVA (50 µg OVA in 50 µl saline, applied directly to nostrils). The i.n. OVA challenge was repeated twice in the two days following the first i.n. OVA challenge. Control cohorts received sham sensitization and challenge with saline. Experimental assessments were made 48 hours after the last OVA challenge.

5.6 BALF collection and analyses

To assess airway inflammation in mice, the whole lung was lavaged to collect bronchoalveolar lavage fluid (BALF). At the experimental end point, mice were anaesthetized with sodium pentobarbital (90 mg/kg, intraperitoneal injection) and tracheostomized with 20-gauge polyethylene catheter inserted and fixed in mid trachea. Lungs were lavaged with 1 mL of cold sterile saline, twice, for a total of 2 mL. The collected BALF was centrifuged at 1100 RPM for 10 min, and the supernatant was isolated and stored at -80 °C. The pellet was re-suspended in 1 mL of cold saline. Cell counts from the re-suspended BALF were estimated using a hemocytometer, and the total BALF cell counts were determined as total number of leukocytes per mL of original BAL. For differential cell counts, cells were spread onto glass slides using a Cytospin® 3 (1000 rpm for 5 mins) (Shandon Inc.) and were stained with a modified Wright-Giemsa stain (Hema 3® Stat Pack, Fisher Scientific). Cell distribution was analyzed by manually identifying and counting eosinophils, lymphocytes, macrophages, and neutrophils in six randomly chosen fields of view examined with a light microscope at 400x magnifications. Cell counts were totaled across the six fields of view, and the ratio was used to calculate the absolute # cells /mL of original BALF.

5.7 Respiratory Mechanics

Mice were anesthetized with sodium pentobarbital (90 mg/kg, intraperitoneal injection) and the trachea was exposed ventrally. A 20-gauge polyethylene catheter was inserted and fixed into the trachea and was further connected to a flexiVent small animal ventilator (Scireq Inc. Montreal, PQ, Canada). Mice were ventilated with a tidal volume of 10 ml/kg body weight, 150 times per min. A positive end expiratory pressure (PEEP) of 3 cmH_2O was used for all studies.

Mice were subjected to an increased dose of nebulized methacholine (MCh) challenge protocol to assess concentration response characteristics of respiratory mechanics. 30μL of saline containing 0 - 50 mg/mL MCh was delivered over 10 seconds using an inline nebulizer at the beginning of each dose point. Low frequency forced oscillation technique was used to assess the effects of MCh challenge on respiratory mechanics. During the low frequency forced oscillation, mechanical ventilation was interrupted, and then a volume perturbation signal was applied using a preset flexiVent Prime-8 protocol. By fitting Zrs to the constant phase model (66,67), the flexiVent software calculated central conducting Newtonian resistance (Rn), peripheral tissue damping (G), tissue elastance or stiffness (H); each parameter was normalized according to body weight. Values for each parameter were calculated as the mean of all 20 perturbation cycles performed after each MCh challenge.

Using the MCh dose curve, airway sensitivity to MCh was quantified by calculating provocative concentration 100 (PC100), dose of nebulized MCh required to elicit 100% increase in baseline Rn. PC100 was calculated using linear regression on dose response curve generated for each mice and was averaged to obtain mean values.

5.8 Lung Histology

Histological assessment was performed using the left lung. Lungs were dissected out and were inflated with 1mL of 10% buffered formalin (pH 7.4) to a pressure of 25 cm H_2O, and fixed for 48 hours prior to tissue processing and paraffin embedding. Paraffin embedded lung specimen were sectioned into 6μm thick serial sections and were stained for Harris Haemotoxylin and Eosin Y (H&E) and Periodic Acid Schiff (PAS) stain. Harris Haemotoxylin and Eosin Y Solution (alcoholic) were purchased from Sigma-Aldrich (St.Loouis, MO) and staining was done following a standard protocol. PAS staining was done using Periodic Acid Schiff Staining System (Sigma-Aldrich, St. Louis, MO) following the manufacturer's protocol. Specimens were viewed and photographed using an upright light microscope equipped with a SPOT CCD camera (Olympus, Canada).

5.9 Goblet cells and mucus score

Twelve large airways (length of basement membrane under epithelium > 1200 μm; columnar epitheliums) from four different animals were assessed for goblet cell metaplasia and mucus production in each exposure group. Based on the ratio of goblet cell area to whole cross-sectional epithelial area, the severity of goblet cell metaplasia and mucus hyper-secretion was scored as previously described (68). In brief, goblet cell metaplasia and mucus secretion was scored from 0 to 3: a score of 0 for no goblet cells, a score of 1 (mild hyperplasia and mucus secretion) for occupation of < 1/3 of the epithelial area by goblet cells with mild mucus secretion, a score of 2 (moderate hyperplasia and mucus secretion) for occupation of ≥ 1/3 to ≤ 2/3 of the epithelial area and moderate mucus secretion; and a score of 3 (severe hyperplasia) for occupation of greater than 2/3 of the epithelial area and copious mucous secretion. The goblet

score was obtained by averaging the scores assigned to airways by two blinded independent observers.

5.10 ELISA: measuring inflammatory cytokine level in whole lung lysate

Left lungs were minced and submerged in 500µL protein lysate RIPA buffer following composition: (Aqueous solution with 10 mM Tris pH 7.5, 150 mM NaCl, 1:100 NP40, 1g/100mL Deoxycholic Acid Salt, 0.1% SDS, 1:100 protease inhibitor cocktail (Sigma-Aldrich, St. Luuis, MO), 1:100 phosphatase inhibitor cocktail 2 (Sigma-Aldrich, St. Louis, MO), and1 mM PMSF, pH adjusted to 8.0). For protein isolation, tissues were thawed, homogenized using a Polytron and were sonicated. Supernatant was collected after centrifugation (13 600x g, 15mins). Protein concentrations were estimated using RC DC™ Protein Assay (BioRad, Hercules, CA) following manufacturer's protocol. Mouse TNF-α ELISA MAX™ Deluxe (BioLegend, San Diego, CA), Mouse IFN-γ ELISA MAX™ Deluxe (BioLegend, San Diego, CA) and Mouse IL-5 ELISA MAX™ Deluxe (BioLegend, San Diego, CA) kits were used with slight modification to manufacturer's protocol. Briefly, ELISA plate preparation was modified for overnight incubation of primary antibodies at 4 °C instead of incubation at 37 °C for 1 hours. 100 uL of protein lysate containing 50ug and 100 ug of total protein were incubated for 20 mins on coated plate. Absorbance at 450 nm was used to read the plates and concentration was estimated using a standard curve on log-log axis.

5.11 qPCR: measuring inflammatory cytokine mRNA abundance

RNA extraction and cDNA Synthesis

Dissected right lungs from each mice were cut into smaller fragments and stored in RNA*later*® (Qiagen, Missisauga, ON, Canada) at -20 °C for up to 6 months. To extract the RNA from the tissues, RNA*later*® was first removed as per manufacture's instructions before the tissue was homogenized using a PowerGen 700 homogenizer (Fisher Scientific), in RLT lysis buffer (Qiagen) and passed through a QIAshredder (Qiagen). RNA was extracted from the tissue lysate using a Qiagen RNeasy® Plus Mini Kit (Qiagen) as per the manufactures instructions, and the supplied gDNA Eliminator Mini Spin Columns were used to remove genomic DNA from the extracted RNA. Assessment of RNA concentration and purity was performed using a spectrophotometer (NanoDrop 2000; Thermo Scientific; Waltham, MA, USA). The qScript™ cDNA SuperMix kit (containing and equimolar ratio of oligo (dT)s and random hexamers) was used for the reverse transcription of RNA (1 μg) to cDNA using the manufacturer's protocol (Quanta BioSciences, Inc., Gaithersburg, MD, USA).

Primer Design & Validation using Polymerase Chain Reaction

Gene sequences were obtained from NCBI (http://www.ncbi.nlm.nih.gov) and input into PrimerQuest (https://www.idtdna.com/Primerquest/) along with intron and exon boundary information for each set of SYBR based qPCR (quantitative polymerase chain reaction) primer set. Verification of output primer sequences involved several *in silico* analysis tools such as UNAFold, PrimerBlast and *in silico PCR* (http://www.idtdna.com/UNAFold; http://www.ncbi.nlm.nih.gov/tools/primer-blast/; http://genome.ucsc.edu/cgi-bin/hgPcr; respectively) and the final primer sequences can be found in Table 5.1. Experimental verification

of primers were done using polymerase chain reaction (PCR); briefly, 1 µL of each 10 µM primer pair, 1 µL of cDNA, 12.5 µL EconoTaq® PLUS GREEN (Lucigen; Middleton, WI, USA) built up to 25 µL with H_2O and processed using a Techne Touchgene Gradient thermocycler (Bibby Scientific Limited; Staffordshire, UK) using the following conditions: initial denaturation of 94 ºC for 5 min, 40 cycles of denaturation, annealing and product extension of 94 ºC 15 sec, 58 ºC for 30 sec and 72 ºC for 35 sec followed by a final extension at 72 ºC for 5 minutes. PCR products were resolved using gel electrophoresis on 2% agarose gels at 70 volts.

qPCR and Data Analysis

Real-time PCR (qPCR) was carried out with the 7500 Real-Time PCR System (Applied Biosystems; Foster City, CA, USA) using primer pairs for eotaxin, ribosomal 18s RNA (18S), interleukin 13 (IL-13), interferon gamma (IFN-γ) and tumor necrosis factor alpha (TNF-α) (Table 5.1). Each qPCR reaction comprised of 12.5 µL SYBR® Green (Applied Biosystems, Warrington, UK), 1 µL of F and 1 µL R primer (10 µM primer stock), 1 µL of cDNA and built up to 25 µL with water before being sealed, briefly centrifuged and run on the thermocycler using the recommended cycling protocol for the SYBR reagent (Applied Biosystems) with a primer annealing temperature of 58 ºC. Product specificity was determined by dissociation curve analysis using the supplied 7500 Sequence Detection software v.1.4 (Applied Biosystems, Foster City, CA, USA). Ribosomal 18s was used as the internal standard with relative gene expression calculated using the ddC_t method as previously described (69).

Table 5.1. Summary of primer sequences utilized in qPCR.

Gene	NCBI Accession #	Primer Sequence	PCR Product Size (bp)
eotaxin	NM_008176.3	F 5'-TTCTATTCCTGCTGCTCACGGTCA R 5'-GGCTTTCAGGGTGCATCTGTTGTT	164
18S	NR_003278	F 5'-CGCCGCTAGAGGTGAAATTC R 5'-TTGGCAAATGCTTTCGCTC	62
IL-13	NM_008355.3	F 5'-GATCTGTGTCTCTCCCTCTGA R 5'-AGGTCCACACTCCATACCA	109
IFN-γ	NM_008337.3	F 5'-GGCCATCAGCAACAACATAAG R 5'-GTTGACCTCAAACTTGGCAATAC	112
TNF-α	NM_013693.3	F 5'-GCCTCCCTCTCATCAGTTCTAT R 5'-CACTTGGTGGTTTGCTACGA	104

Primers were designed using Primer Quest (IDT.com) and initially verified *in silico* using Primer Blast (NCBI), UNA Fold (IDT) and *in silico* PCR (UCSC) before being confirmed with standard PCR and 1D electrophoresis. All primer sets were also tested using PCR. Abbreviations used: ribosomal 18s RNA (18S), interleukin 13 (IL-13), interferon gamma (IFN-γ) and tumor necrosis factor alpha (TNF-α)

5.12 Statistical Analysis

All statistical analysis was carried out using IBM SPSS 20 software and/or GraphPad Prism 6. Results are expressed as mean ± standard error of the mean (SEM). Analysis of variance (ANOVA) was used to compare the means. Normality of the data was assessed by examining bar histograms generated using IBM SPSS 20. Data were log transformed to log base 10 when found positively skewed; respiratory mechanics and ddC_t for qPCR were log transformed. Levene's test was performed to assess equality of variance where appropriate. One-way ANOVA, followed by the Bonferroni post hoc, was used to compare means of PC100, total cell counts, and ddC_t for qPCR analysis. Two-way ANOVA followed by Tukey's post hoc test was used to compare the means for respiratory mechanics. The Kruskal-Wallis test, followed by Dunn's Multiple Comparison, was used to compare the mucus score. P-values less than 0.05 were considered statistically significant unless noted otherwise.

6. RESULTS

6.1 PFOA is detectable in serum after both PFOA and FTOH exposure

To determine the effectiveness of the exposure protocol, serum levels of PFOA were measured in mice exposed to either PFOA (by ingestion) or FTOH (by inhalation) beginning *in utero* and extending through 11-12 weeks of age (Fig. 6.1). While PFOA was detected in only trace amounts in the serum of naïve (untreated) animals (1.75 ± 0.21 ng/mL), strongly detectable levels were measured in serum from mice exposed to either compound (Fig. 6.1). Serum PFOA concentrations in PFOA and FTOH-exposed mice were 4800 ± 1100 ng/mL and 5400 ± 900 ng/mL, respectively. There was no statistical difference in serum PFOA concentration between the two groups ($p > 0.05$).

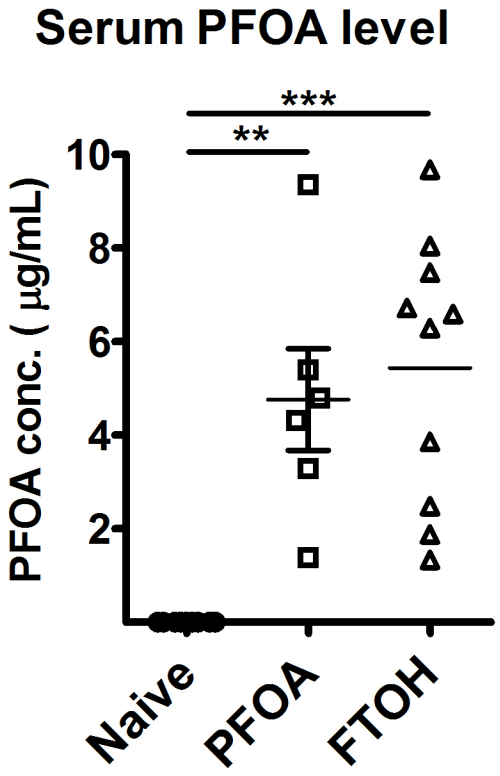

Fig 6.1. *Serum concentrations of PFOA measured in PFOA or FTOH exposed mice using LC-MS/MS.* Animals were exposed to PFOA through direct ingestion of PFOA in diet or through bioconversion of inhaled FTOH to PFOA. Chemical exposure began *in utero* and continued through postnatal. Serum PFOA concentration was measured at the experimental endpoint when mice were 11 to 12 weeks old. Error bars represent the standard error mean. Statistical significance was determined using ANOVA; $P < 0.01$**(**)** and $P < 0.001$**(***)**.

6.2 PFOA and PFOS ingestion resulted in increased body weight and liver enlargement

Exposure to dietary PFOA and PFOS correlated with significant weight gain and liver enlargement (Fig 6.2). At 11 - 12 weeks of age, PFOA- and PFOS-exposed animals had mean body weights that were 13% and 9% greater than the naïve, respectively (Table 6.1). The two groups also had 80% and 44% greater liver weight to body weight ratio than the naïve, respectively (Table 6.1). However, neither weight gain nor liver enlargement was observed in mice that inhaled FTOH. OVA sensitization and challenge also had no detectable impact on the body and liver weights. Mean values are the average of more than 12 mice per group.

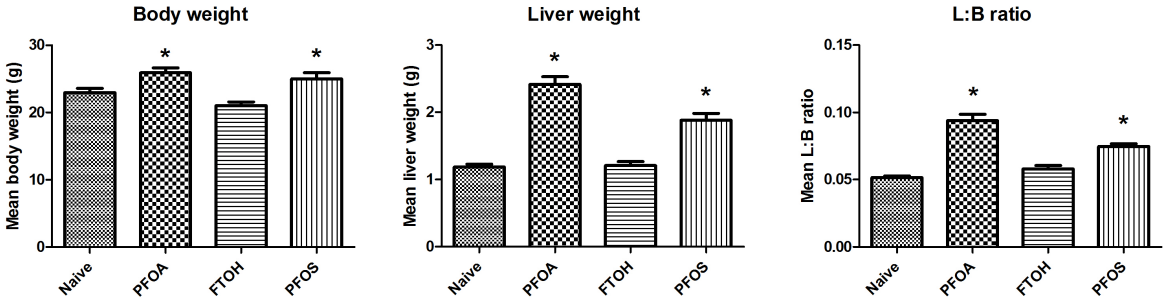

Fig 6.2. *Ingestion of PFOA or PFOS induced weight gain and liver enlargement in mice.* Body and wet liver weight was measured at age 11-12 weeks. * denotes significant statistical difference compared to the naïve values (ANOVA, $p<0.05$). n >12 per group. Error bars represent SEM.

Table 6.1. Body and liver weights and liver weight to body weight ratio of the PFCs exposed mice measured at the experimental endpoint, 11-12 weeks of age

	Body weight (g)	Liver weight (g)	Liver weight/Body weight
Naïve	22.94 ± 0.63	1.18 ± 0.04	0.052 ± 0.001
PFOA	25.88 ± 0.76*	2.42 ± 0.11*	0.094 ± 0.005*
FTOH	21.02 ± 0.54	1.21 ± 0.06	0.057 ± 0.002
PFOS	24.99 ± 0.89*	1.88 ± 0.11*	0.075 ± 0.002*

Values are means ± SE. L:B ratio, liver to body weight ratio. (*) indicates significant difference compared to the naïve values (ANOVA, $P<0.05$).

6.3 PFC exposure had no detectable impact on baseline lung function

Respiratory mechanics were measured in PFOA-, FTOH- and PFOS-exposed mice using a flexiVENT small animal ventilator at 11-12 weeks of age. Six mechanical parameters were assessed prior to methacholine (MCh) challenge: respiratory resistance (R); elastance (E); compliance (C); Newtonian resistance (Rn); tissue damping (G); and tissue elastance (H). There was no detectable change in any parameters at baseline, in any PFC-exposed group compared to naïve (ANOVA, $p>0.05$) (Fig. 6.3, Table 6.2).

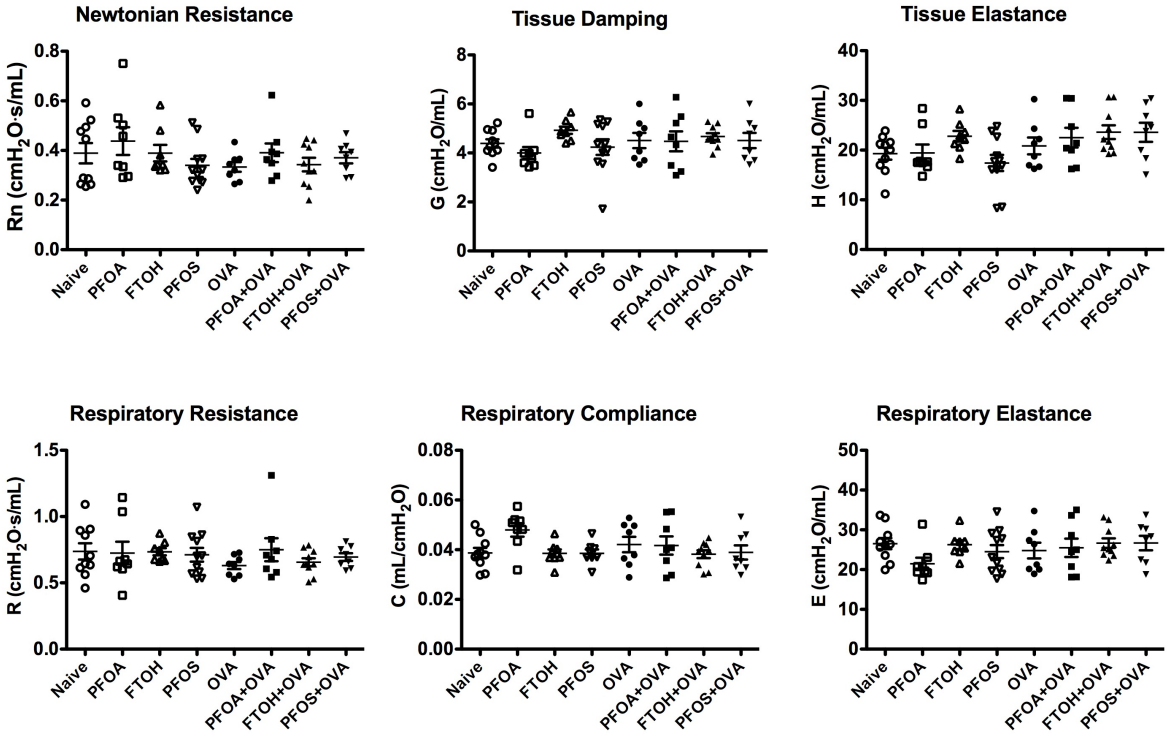

Fig 6.3. *In-utero-through-postnatal chronic exposures to PFOA, FTOH or PFOS do not alter baseline respiratory mechanics*. Lung function was assessed at 11 to 12 weeks of age using a flexiVent small animal ventilator. Parameters measured are: respiratory resistance; elastance; compliance; airway resistance; tissue damping; and tissue elastance. No significant statistical difference was present in any comparison ($p>0.05$).

6.4 Life-long exposure to PFOA, but not PFOS, induced airway hyperresponsiveness

Interestingly, lifetime exposure to ingested PFOA and inhaled FTOH induced airway hyperresponsiveness (AHR), as indicated by the left-upward shift of the MCh dose-response curves (Fig. 6.4). Central conducting airways in PFOA- and FTOH-exposed mice were hyperreactive to MCh challenge, generating greater maximum Newtonian resistance: the maximum Rn, measured at the maximum experimental MCh dose ([MCh] = 50 mg/mL), was significantly greater in the PFOA- and FTOH-exposed mice than in the naïve animals (**max Rn**: PFOA 1.68 ± 0.19 $cmH_20 \cdot s \cdot mL^{-1}$, FTOH 1.87 ± 0.23 $cmH_20 \cdot s \cdot mL^{-1}$, Naïve 1.02 ± 0.12 $cmH_20 \cdot s \cdot mL^{-1}$; ANOVA, $p<0.05$; Table 6.3). Indeed, Rn measured in the PFOA- and FTOH-exposed mice were significantly higher than that of the naïve at every MCh dose greater than 12 mg/mL (two-way ANOVA pairwise comparison, $P<0.05$). At the same time, PFOA- and FTOH-exposed mice were hypersensitive to MCh, indicated by the significantly lower PC100 in the PFOA- and FTOH-exposed mice compared to the naïve (**PC100**: PFOA 13.0 ± 3.8 mg/mL, FTOH 12.2 ± 1.7 mg/mL, Naïve 41.6 ± 9.0 mg/mL; ANOVA $p<0.05$; Table 6.3). Taken together, the hyperreactive and hypersensitive airways in PFOA- and FTOH-exposed mice constitute AHR. Of note, the degree of AHR was comparable to the OVA-induced AHR measured in OVA-only group (Compare Fig. 6.4A & 6.5B). In PFOS exposed animals, airways were hypersensitive to MCh, as indicated by the significant decrease in PC100 (**PC100**: PFOS 17.8 ± 3.9 mg/mL vs Naïve 41.6 ± 9.0 mg/mL; ANOVA, $p<0.05$; Table 6.3), but there was no detectable increase in the maximum Rn compared to the naïve.

Tissue damping (G), which is closely related to peripheral tissue resistance, was measured after the maximum experimental MCh challenge ([MCh] = 50 mg/mL). This G value was significantly greater in the PFOA-exposed mice than in the naïve (**G_{max}**: PFOA 20.67 ± 2.20

$cmH_20 \cdot mL^{-1}$; FTOH Naïve 11.27 ± 1.23 $cmH_20 \cdot mL^{-1}$, $p<0.05$; Table 6.4). Tissue elastance (H) was also greater in PFOA- and FTOH-exposed mice at the maximum MCh dose compared to the naïve ($\mathbf{H_{max}}$: PFOA 69.70 ± 6.27 $cmH_20 \cdot mL^{-1}$, FTOH 64.72 ± 9.80 $cmH_20 \cdot mL^{-1}$, vs Naïve 37.56 ± 4.20 $cmH_20 \cdot mL^{-1}$, two-way ANOVA, $P<0.05$; Table 6.5).

Finally, tissue hysteresivity (*eta*), which characterizes the ratio of energy dissipation to energy conservation in the lung tissues, was evaluated. A change in baseline eta reflects inhomogeneity in the lungs or structural changes in the airways. In our study, there were no detectable changes in *eta* in any one of the PFC exposed cohorts (Table 6.2).

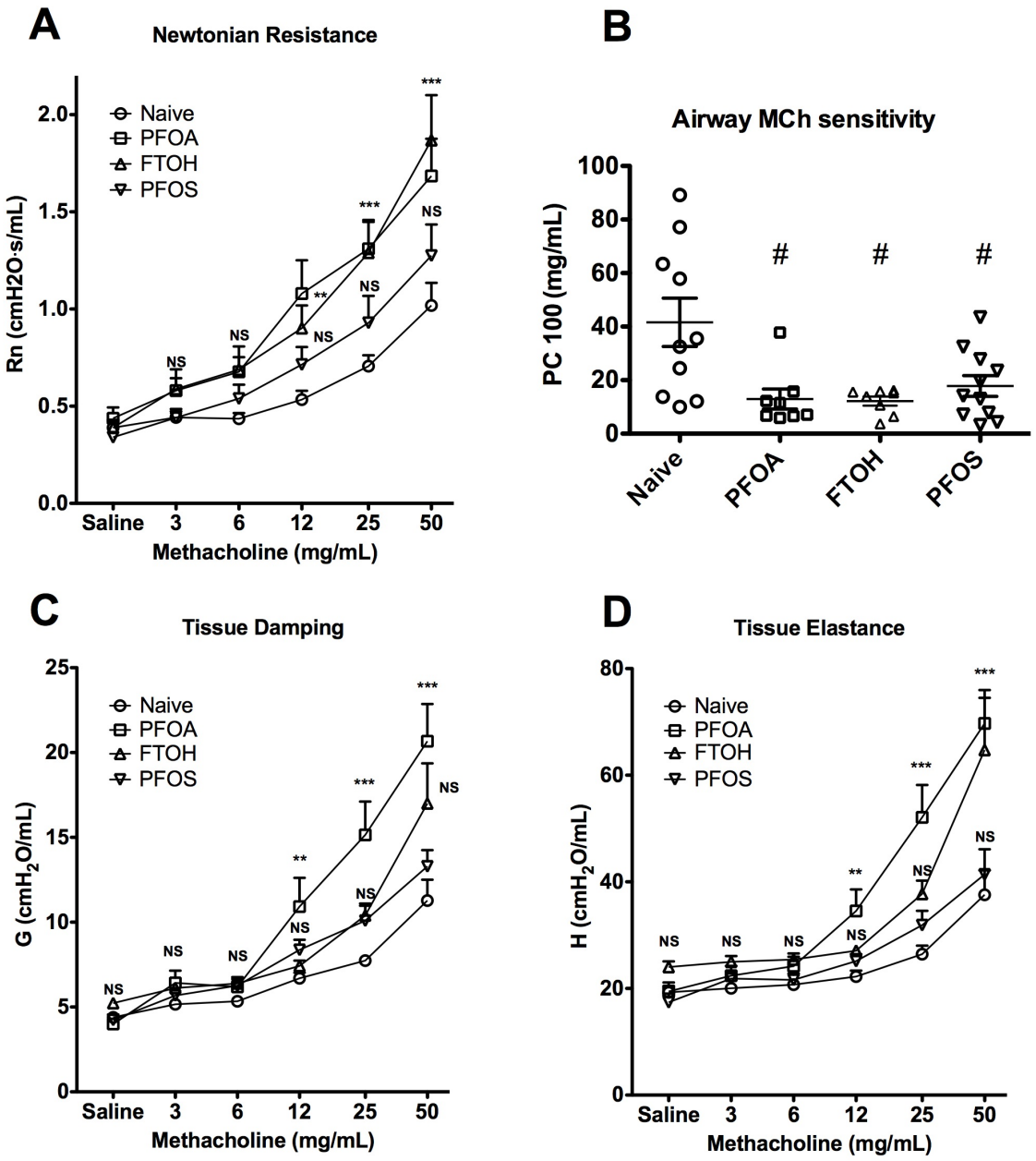

Fig 6.4. *Chronic exposure of mice to ingested PFOA or inhaled FTOH induced airway hyperresponsiveness in 12 weeks old Balb/c mice.* Airway mechanics were assessed using flexiVent® system after mice inhaled increasing doses of nebulized methacholine (MCh)(0 - 50 mg/mL). Methacholine (dose-response curve for **(A)** Newtonian resistance (Rn); **(c)** tissue damping (G); and **(D)** tissue elastance (H) are plotted for each group. **(B)** Central airway MCh sensitivity was quantified by calculating provocative concentration 100 (PC100), a concentration of MCh required to elicit 100% increase in baseline Rn. Means were compared with that of the naïve using two-way ANOVA, and the difference was considered significant if $P < 0.05$ **(*),** $P < 0.01$**(**)** and $P < 0.001$**(***)** and not significant (NS) if $p > 0.05$. # indicates significant statistical difference compared to 5the naïve (One-way ANOVA, $p < 0.05$). Error bars shown represent the standard error of mean (±SEM). The number of animals per group was 8-10.

Table 6.2. Baseline respiratory mechanic parameters measured in PFOA-, FTOH- and PFOS-exposed mice

	Rn baseline ($cmH_20 \cdot s \cdot mL^{-1}$)	G baseline ($cmH_20 \cdot mL^{-1}$)	H baseline ($cmH_20 \cdot mL^{-1}$)	eta (G/H)
Naïve (n=10)	0.389 ± 0.041	4.389 ± 0.222	19.28 ± 1.09	0.24 ± 0.02
PFOA (n=8)	0.438 ± 0.056	3.998 ± 0.246	19.44 ± 1.68	0.21 ± 0.01
FTOH (n=8)	0.389 ± 0.033	5.231 ± 0.121	24.03 ± 1.06	0.22 ± 0.01
PFOS (n=11)	0.340 ± 0.026	4.239 ± 0.319	17.41 ± 1.62	0.27 ± 0.04
OVA-only (n=8)	0.334 ± 0.020	4.510 ± 0.310	20.85 ± 1.70	0.22 ± 0.01
PFOA+OVA (n=8)	0.391 ± 0.038	4.475 ± 0.407	22.51 ± 1.98	0.20 ± 0.01
FTOH+OVA (n=11)	0.343 ± 0.027	4.672 ± 0.134	23.61 ± 1.38	0.20 ± 0.01
PFOS+OVA (n=8)	0.371 ± 0.022	4.598 ± 0.183	23.57 ± 1.92	0.20 ± 0.01

Values are mean ± SE. Rn, Newtonian resistance; G, tissue damping; H, tissue elastance; eta, tissue hysteresivity. There was no statistical significant difference between chemical exposed group and naïve ($P>0.05$).

Table 6.3. Newtonian resistance measured in mice exposed to PFOA, FTOH or PFOS

	Rn baseline ($cmH_20 \cdot s \cdot mL^{-1}$)	Rn maximum ($cmH_20 \cdot s \cdot mL^{-1}$)	PC 100 (mg/mL)
Naïve (n=10)	0.389 ± 0.041	1.02 ± 0.12	41.6 ± 9.0
PFOA (n=8)	0.438 ± 0.056	1.68 ± 0.19 †	13.0 ± 3.8 †
FTOH (n=8)	0.389 ± 0.033	1.87 ± 0.23 †	12.2 ± 1.7 †
PFOS (n=11)	0.340 ± 0.026	1.27 ± 0.16	17.8 ± 3.9 †

Values are mean ± SE. Rn, Newtonian resistance; PC 100, provocative concentration 100. **(†)** indicates significant difference compared to naïve ($P<0.05$).

Table 6.4. Tissue damping measured in mice exposed to PFOA, FTOH or PFOS

	G baseline ($cmH_20 \cdot mL^{-1}$)	G maximum ($cmH_20 \cdot mL^{-1}$)
Naïve (n=10)	4.389 ± 0.222	11.27 ± 1.23
PFOA (n=8)	3.998 ± 0.246	20.67 ± 2.20 †
FTOH (n=8)	5.231 ± 0.121	17.00 ± 2.36
PFOS (n=11)	4.239 ± 0.319	13.29 ± 0.95

Values are mean ± SEM. G, tissue damping. **(†)** indicates significant difference compared to the naïve (ANOVA, $P<0.05$).

Table 6.5. Tissue elastance measured in mice exposed to PFOA, FTOH or PFOS

	H baseline ($cmH_20 \cdot mL^{-1}$)	H maximum ($cmH_20 \cdot mL^{-1}$)
Naïve (n=10)	19.68 ± 1.21	37.56 ± 4.20
PFOA (n=8)	19.44 ± 1.68	69.70 ± 6.27 †
FTOH (n=8)	24.03 ± 1.06	64.72 ± 9.80 †
PFOS (n=11)	17.41 ± 1.62	41.38 ± 4.74

Values are mean ± SEM. H, tissue elastance. **(†)** indicates significant difference compared to the naïve (ANOVA, P<0.05).

6.5 PFOA and FTOH exposure did not augment allergen induced AHR

The observation that *in-utero*-through-postnatal exposure to PFOA or FTOH induced AHR in mice led to the question of whether allergic AHR would be worsened by the altered lung mechanics resulting from the lifelong exposure to PFOA or FTOH. To answer this key question, some PFC-exposed mice were sensitized and challenged with ovalbumin (OVA) and lung function was assessed.

OVA sensitization and challenge consistently established allergen-induced AHR in the controls, as indicated by the 93% increase in maximum Rn (**max Rn**: OVA-only 1.97 ± 0.18 $cmH_20 \cdot s \cdot ml^{-1}$ vs Naïve 1.02 ± 0.12 $mH_20 \cdot s \cdot ml^{-1}$; $p<0.05$, Table 6.5) and 82% decrease in PC 100 (**PC100:** OVA-only 7.3 ± 0.4 mg/ml vs Naïve 41.6 ± 9.0 mg/ml; $p<0.05$, Fig. 6.5B, Table 6.5). PFOA-, FTOH- or PFOS-exposed mice that were sensitized and challenged with OVA also exhibited AHR, but no further augmentation of AHR beyond the level achieved by OVA-only treatment was observed in any group exposed to PFCs; the magnitude of maximum Rn in any of the PFCs + OVA groups was not different compared to that of the OVA-only group (**max Rn**: PFOA + OVA 1.73 ±0.24 $cmH_20 \cdot s \cdot mL^{-1}$, FTOH + OVA 1.70 ± 0.22 $cmH_20 \cdot s \cdot mL^{-1}$, PFOS + OVA 1.89 ± 0.25 $cmH_20 \cdot s \cdot mL^{-1}$; ANOVA, $p>0.05$;Table 6.5, Fig. 6.5 A). PC100 was also not different in any PFCs + OVA groups compared to the OVA-only (**PC100**: PFOA + OVA 5.8 ±

1.7 mg/mL, FTOH + OVA 11.6 ± 1.8 mg/mL, PFOS + OVA 9.6 ± 1.6 mg/mL vs OVA-only 7.3 ± 0.4 mg/mL; P>0.05;Table 6.5, Fig 6.5 B).

Interestingly, PFOA+OVA group exhibited concentration response characteristics of tissue damping (G) that deviated from that of OVA-only groups (Fig. 6.5 C). The maximum G, measured after inhalation of 50 mg/mL of MCh, was significantly greater in the PFOA+OVA group compared to the OVA-only group (**max G:** PFOA + OVA 38.0 ± 7.6 $cmH_20 \cdot mL^{-1}$ vs OVA-only 26.3 ± 2.6 $cmH_20 \cdot mL^{-1}$, $p<0.05$;Table 6.6, Fig. 6.5 B), indicating augmented airflow limitation in the periphery when mice were co-exposed to PFOA and OVA. However, PFOA+OVA, PFOS+OVA, and FTOH+OVA exposure elicited no detectable impact on the tissue elastance (H) beyond the level achieved with OVA-only (Fig. 6.5 D).

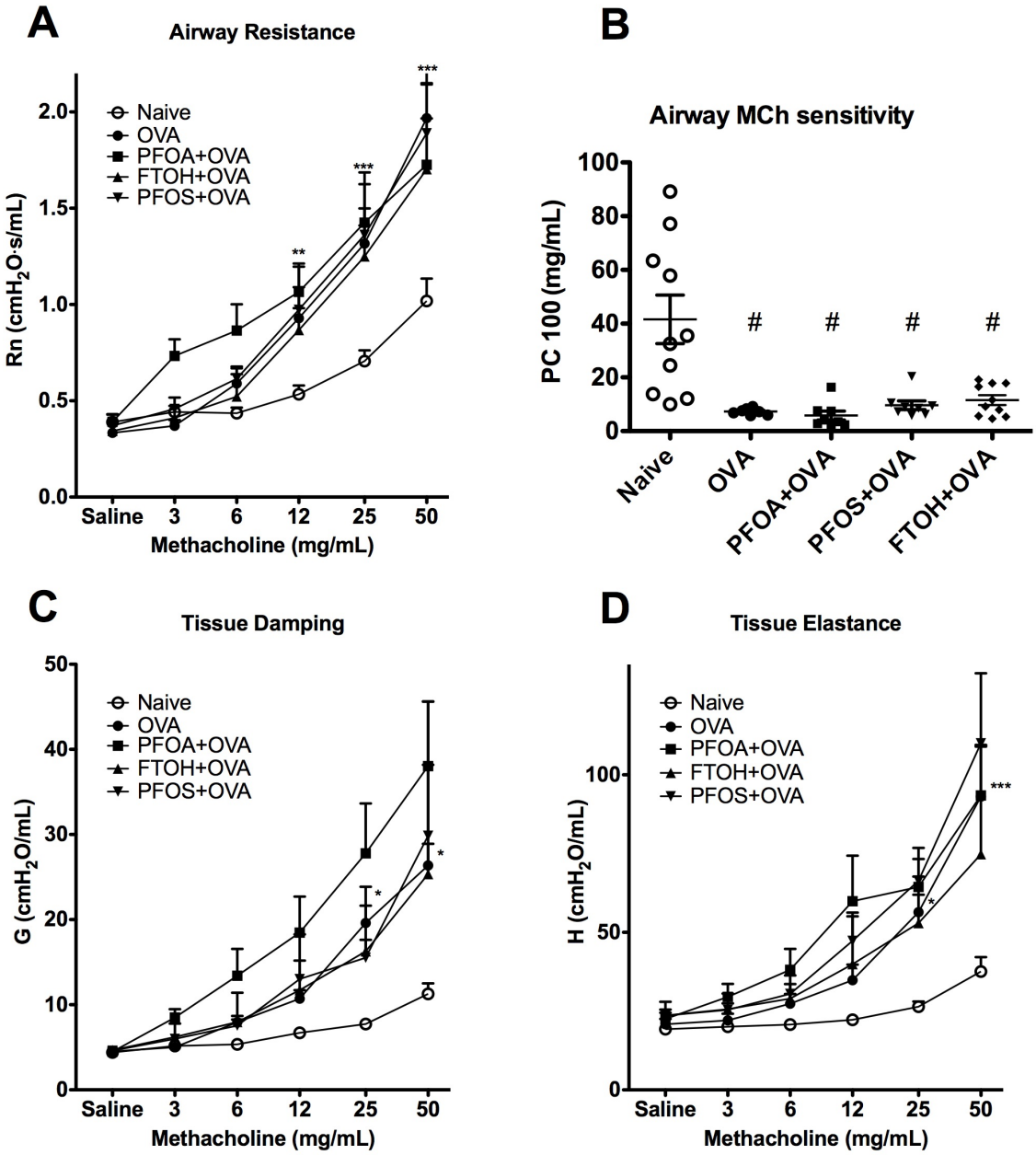

Fig 6.5. *Chronic exposure of mice to PFOA, FTOH or PFOS did not further augment ovalbumin-induced airway hyperresponsiveness.* Airway mechanics were assessed using flexiVent® system after mice inhaled increasing doses of nebulized methacholine (MCh) (0-50 mg/mL). MCh dose-response curve for **(A)** Newtonian resistance (Rn); **(C)** tissue damping (G); and **(D)** tissue elastance (H) are plotted for each group. **(B)** MCh sensitivity of conducting airways was quantified by calculating provocative concentration 100 (PC100), a concentration of MCh required to elicit 100% increase in baseline Rn. * ($P < 0.05$), ** ($P < 0.01$) and *** ($P < 0.001$) indicate statistical difference between the OVA-only animals and the unexposed naïve animals (two-way ANOVA). # indicates significant difference compared to the naïve (one-way ANOVA, $P<0.05$). Error bars shown represent the standard error of mean (±SEM). The number of animals per group was 8-10.

Table 6.6. Newtonian resistance measured in mice that were exposed to PFOA, FTOH or PFOS and were also sensitized and challenged with ovalbumin

	Rn baseline ($cmH_20 \cdot s \cdot ml^{-1}$)	Rn maximum ($cmH_20 \cdot s \cdot ml^{-1}$)	PC 100 (mg/ml)
Naïve (n=10)	0.389 ± 0.041	1.02 ± 0.12†	41.6 ± 9.0†
OVA-only (n=8)	0.334 ± 0.020	1.97 ± 0.18	7.3 ± 0.4
PFOA + OVA (n=8)	0.391 ± 0.038	1.73 ±0.24	5.8 ± 1.7
FTOH + OVA (n=11)	0.343 ± 0.027	1.70 ± 0.22	11.6 ± 1.8
PFOS + OVA (n=8)	0.371 ± 0.022	1.89 ± 0.25	9.6 ± 1.6

Values are mean ± SE. OVA, ovalbumin; Rn, Newtonian resistance; PC 100, provocative concentration 100 **(**†**)** indicates significant difference compared to OVA-only (P<0.05).

Table 6.7. Tissue damping measured in mice that were exposed to PFOA, FTOH or PFOS and were also sensitized and challenged with ovalbumin

	G baseline ($cmH_20 \cdot ml^{-1}$)	G maximum ($cmH_20 \cdot ml^{-1}$)
Naïve (n=10)	4.389 ± 0.222	11.27 ± 1.23†
OVA-only (n=8)	4.510 ± 0.310	26.36 ± 2.55
PFOA+OVA(n=8)	4.475 ± 0.407	38.03 ± 7.60†
FTOH+OVA (n=11)	4.672 ± 0.134	25.34 ± 6.41
PFOS+OVA (n=8)	4.598 ± 0.183	29.86 ± 8.34

Values are mean ± SE. G, tissue damping. **(**†**)** indicates significant difference compared to OVA-only (P<0.05).

Table 6.8. Tissue elastance measured in mice that were exposed to PFOA, FTOH or PFOS and were also sensitized and challenged with ovalbumin

	H baseline ($cmH_20 \cdot mL^{-1}$)	H maximum ($cmH_20 \cdot mL^{-1}$)
Naïve (n=10)	19.68 ± 1.21	37.56 ± 4.20†
OVA-only (n=8)	20.85 ± 1.70	93.09 ± 16.12
PFOA+OVA(n=8)	22.50 ± 1.98	93.45 ± 11.49
FTOH+OVA (n=11)	23.61 ± 1.38	74.82 ± 10.97
PFOS+OVA (n=8)	23.57 ± 1.92	110.03 ± 22.22

Values are mean ± SEM. H, tissue elastance; PC 100, concentration of methacholine required to double the baseline G. i.e. provocative concentration 100. **(**†**)** indicates significant difference compared to the naïve values (ANOVA, P<0.05).

6.6 FTOH and PFOS exposure blunted OVA induced leukocyte infiltration to the lungs

Because PFCs have the potential to modulate immune responses, the impact of chronic exposure of mice to PFOA, FTOH or PFOS on airway inflammation was assessed. The BALF collected from mice exposed to PFCs was analyzed to assess leukocyte infiltration of the lungs, by counting the total inflammatory cell number and distribution. Interestingly, mice that ingested PFOA exhibited 25-fold higher total cell count compared to the naïve (**total leukocytes number in BALF:** PFOA (58.1 ± 10.8) $x10^4$ cells/mL BALF vs naïve (2.28 ± 0.17) $x10^4$ cells/mL BALF, $p<0.05$; Table 6.7), but this effect was not observed in the mice exposed to inhaled FTOH, a treatment which resulted in a similar serum PFOA concentration as those ingested PFOA in diet (Fig. 6.1). The increase in total cell count was associated with an increase in macrophage number in the BALF and increased *TNF- α* mRNA abundance. Moreover, there was an increase in *IL-13, IFN-γ* mRNA abundance in the lungs exposed to dietary PFOA and PFOS (Fig. 6.9; Table 6.10).

Airway inflammation was further assessed for goblet cell hyperplasia, in large conducting airways (airway cross-section area > 1200 μm^2), using semi-quantitative histological assessment. No detectable goblet cell hyperplasia was observed histologically in any one of PFC-only exposed groups (Fig. 6.8; Table 6.8).

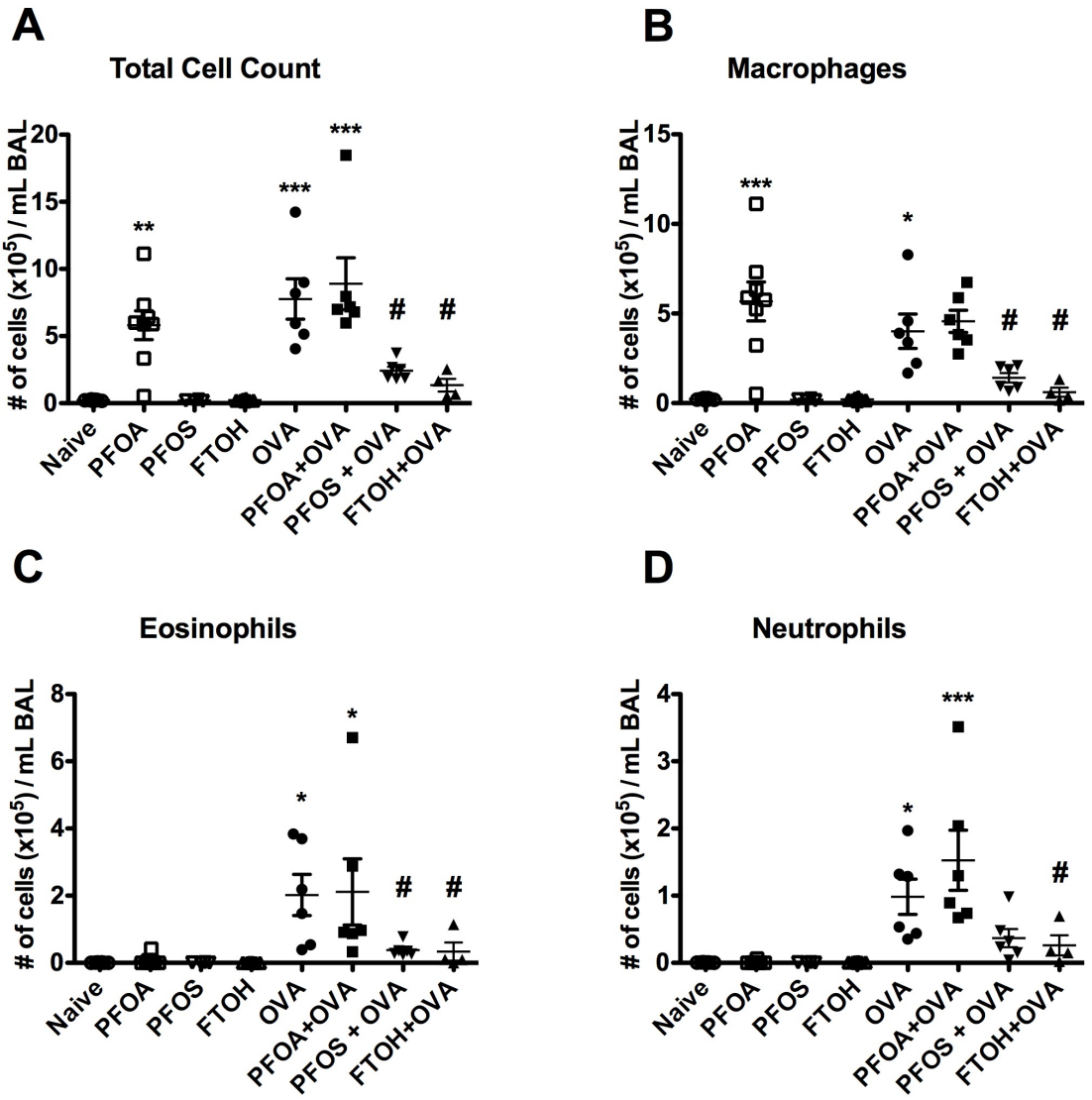

Fig 6.6. *Inflammatory cell counts in bronchoalveolar fluid (BALF).* BALF was collected from Balb/c mice at 12 weeks of age. Prior to the collection, all mice were anesthetized and mechanically ventilated for approximately 30 minutes to assess respiratory mechanics. **(A)** Total cell counts in BALF were estimated using hemocytometer, and values are expressed as # cells / mL of obtained BALF. 200uL of BALF was cytospun and fixed on a coverslip and stained with a modified Wright-Giemsa stain. Cell distribution was analyzed by manually identification of **(B)** macrophage, **(C)** eosinophils, **(D)** neutrophils in six randomly chosen fields of view examined with a light microscope at 400x magnifications. Mean values were compared against that of the naïve using ANOVA, and the difference was considered significant if $P < 0.05$ **(*)**, $P < 0.01$**(**)** and $P < 0.001$**(***)**, or not significant if $P > 0.05$ **(NS).** # indicate significant differences in the mean compared to OVA-only group. Error bars shown represent the standard error of mean (±SEM). Number of animals per group was 6-8.

We further assessed whether the chemical exposure impacted allergen induced airway inflammation. PFC-exposed mice were sensitized and challenged with ovalbumin (OVA) and BALF was collected for analysis. OVA sensitization and challenge resulted in a dramatic infiltration of leukocytes in the lungs as reflected by an increase in total cell count in BALF (**total leukocytes number in BALF:** OVA-only (77.6 ± 15.0) $x10^4$ cells/mL BALF vs. naïve (2.28 ± 0.17) $x10^4$ cells/mL BALF, $p<0.05$). Furthermore, there was significantly elevated leukocyte number in peribronchiole regions (Fig. 6.7), and significant goblet cell hyperplasia in conducting airways (Fig. 6.7 and Table 6.9).

Surprisingly, allergen induced leukocyte infiltration in the lungs was blunted by exposure to FTOH or PFOS, but not to PFOA. FTOH exposure decreased the total cell count in BALF by 83% ($p<0.05$) compared to OVA-only. The decrease in the total cell was associated with 85% ($p<0.05$), 83% ($p<0.05$) and 73% ($p<0.05$) decrease in the macrophage, eosinophil and neutrophil numbers, respectively. Similarly, PFOS exposure decreased the total cell count in BALF by 61% ($p<0.05$) compared to OVA-only, and it was associated with 65% ($p<0.05$) decreases in macrophage numbers (Fig. 6.6). However, histological assessment of goblet cell and mucus abundance revealed no detectable changes in OVA-induced goblet cell hyperplasia by PFOA, FTOH and PFOS (Fig. 6.8;Table 6.9).

We then attempted to assay cytokine abundance in BALF by enzyme-linked immunosorbent assay (ELISA) in collaboration with Dr. John Gordon at the University of Saskatchewan. Due to inconsistency in the measurement output and low abundance of some cytokines in BALF, BALF samples were exhausted before any reliable data were generated. So, we then attempted to measure level of IL-5, TGF-β and IFN-γ in the whole lung lysate as described in the methods. This was also unsuccessful with no consistence and reliable data

generated; absorbance values coincided in the lower end of standard curve close to that of a blank-well with no consistency between experimental or biological replicates (Table 6.13). This likely resulted from RIPA buffer containing protease and phosphotase inhibitor may not be compatible with ELISA reaction. Alternatively, there may have been too low abundance of cytokine relative to amount of whole lung protein.

Finally with success, we measured mRNA abundance of *eotaxin, IL-13, IFN-* γ and *TNF-* α in whole lung using qPCR. Consistent with the presence of eosinophils in the BALF, we detected elevated level of *eotaxin* and *IL-13* in OVA challenged lungs (Fig. 6.9A&D). Interestingly, mRNA level of *IFN-* γ was elevated in both PFOA and PFOS exposed group (Fig. 6.9 C) and this effect was retained in PFCs exposed mice that were also sensitized and challenged with OVA. *TNF-* α level was increased in OVA-only and PFOA+OVA group, but the same effects weren't demonstrated in the PFOS+OVA group. Unfortunately, we weren't able to assess mRNA level in FTOH exposed mice because a routine RNA sample preservation was implemented after FTOH exposed mice groups were already sacrificed.

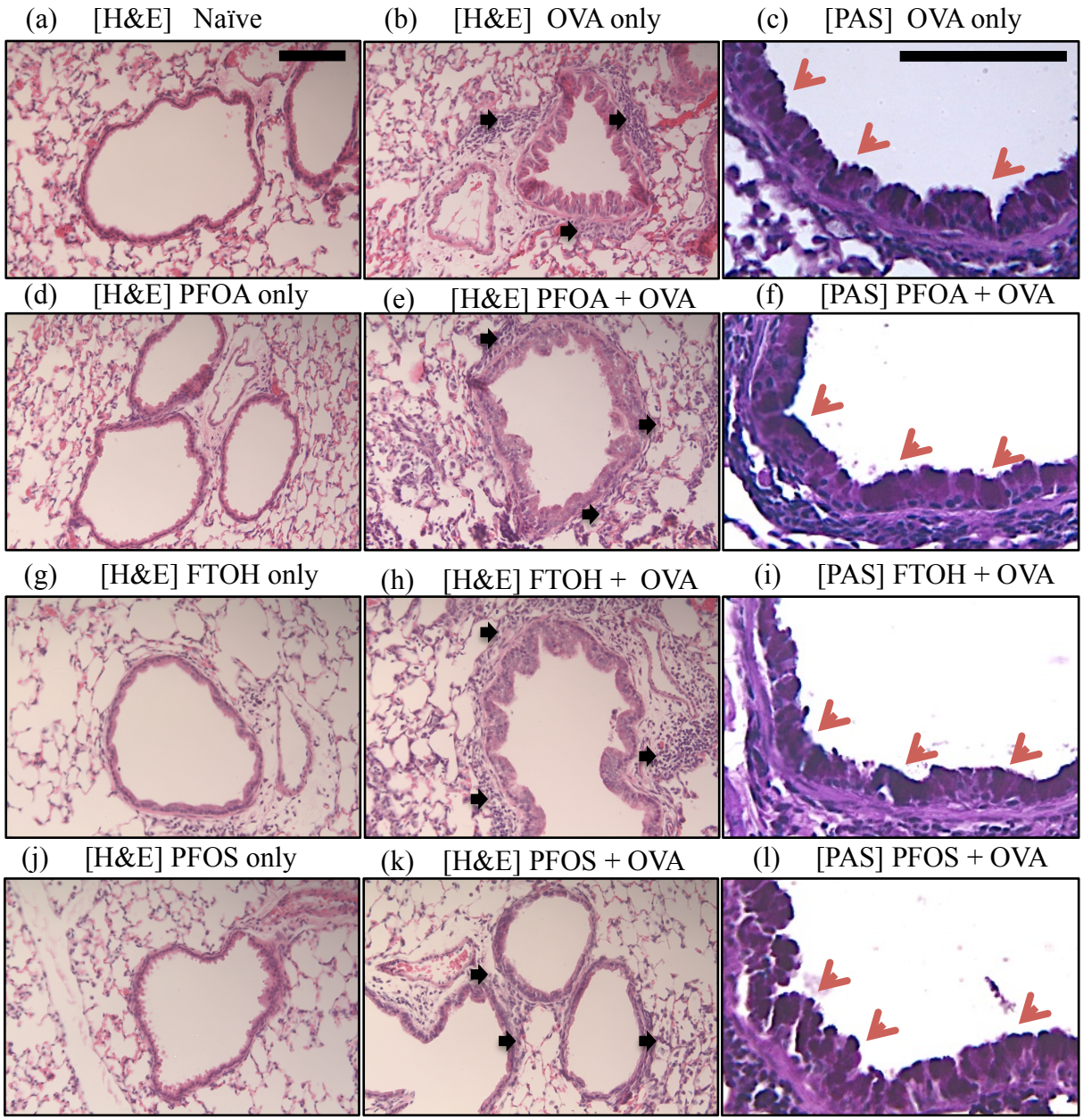

Fig 6.7. *Histology of left lungs of Balb/c mice exposed to PFCs.* **(a,b,c)** mice with no exposure to PFCs; **(d,e,f)** mice exposed to ingested PFOA; **(g,h,i)** mice exposed to inhaled FTOH; **(j,k,l)** mice exposed to ingested PFOS. PFCs exposure started *in utero* at gestation day two and continued through and after weaning. Pups were kept on same diet and housing condition until they were sacrificed at 11-12 weeks of age (20-24g body weight). Histology sections were stained with **(LEFT & MIDDLE)** hematoxylin and eosin (H&E) stain and **(RIGHT)** Periodic-acid Schiff (PAS) stain. **(MIDDLE & Right)** mice were sensitized and challenged with ovalbumin (OVA) in the final three weeks of the study and were sacrificed at 11-12 weeks of age (20-24g body weight). Black scale bar is equal to 100 µm. **(RED ARROW HEADS)** point to goblet cells and mucus in the airway epithelium. **(BLACK ARROWS)** point to peri-bronchial inflammation with infiltrating leukocytes.

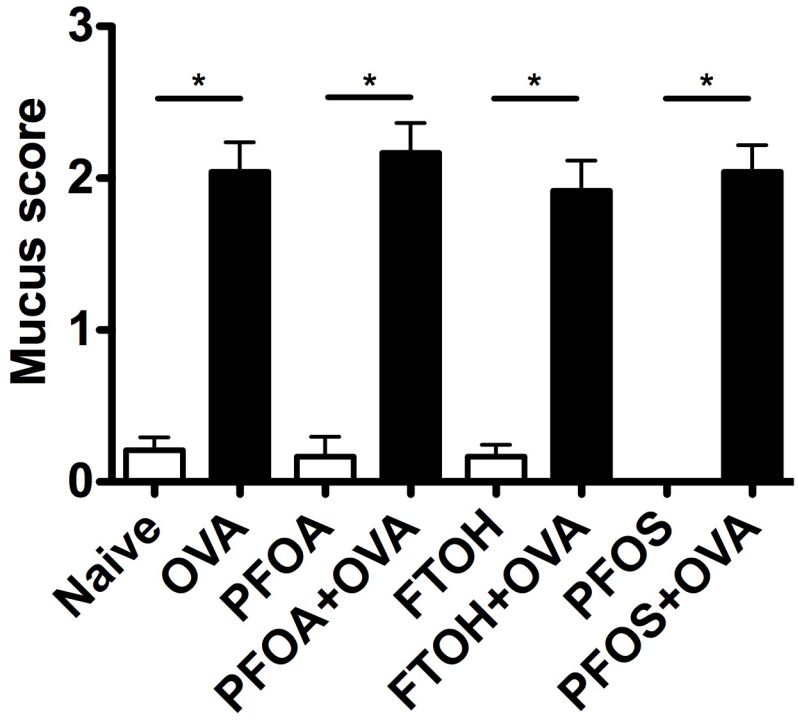

Fig 6.8. *Goblet cell and mucus score in PFC exposed animals - with and without OVA sensitization and challenge - show no detectable impact of PFCs exposures on allergen induced goblet cell hyperplasia.* Mean scores are the average of scores from twelve conducting airways from four different animals. Two independent observers scored each airway. Goblet cell metaplasia and mucus secretion was scored from 0 to 3; 0 indicating no presence of goblet cell while 3 indicate severe goblet cell hyperplasia with greater than 2/3 of the airway epithelial stained with Periodic Acid Schiff stain. **(*)** indicates a significant difference with $p<0.05$.

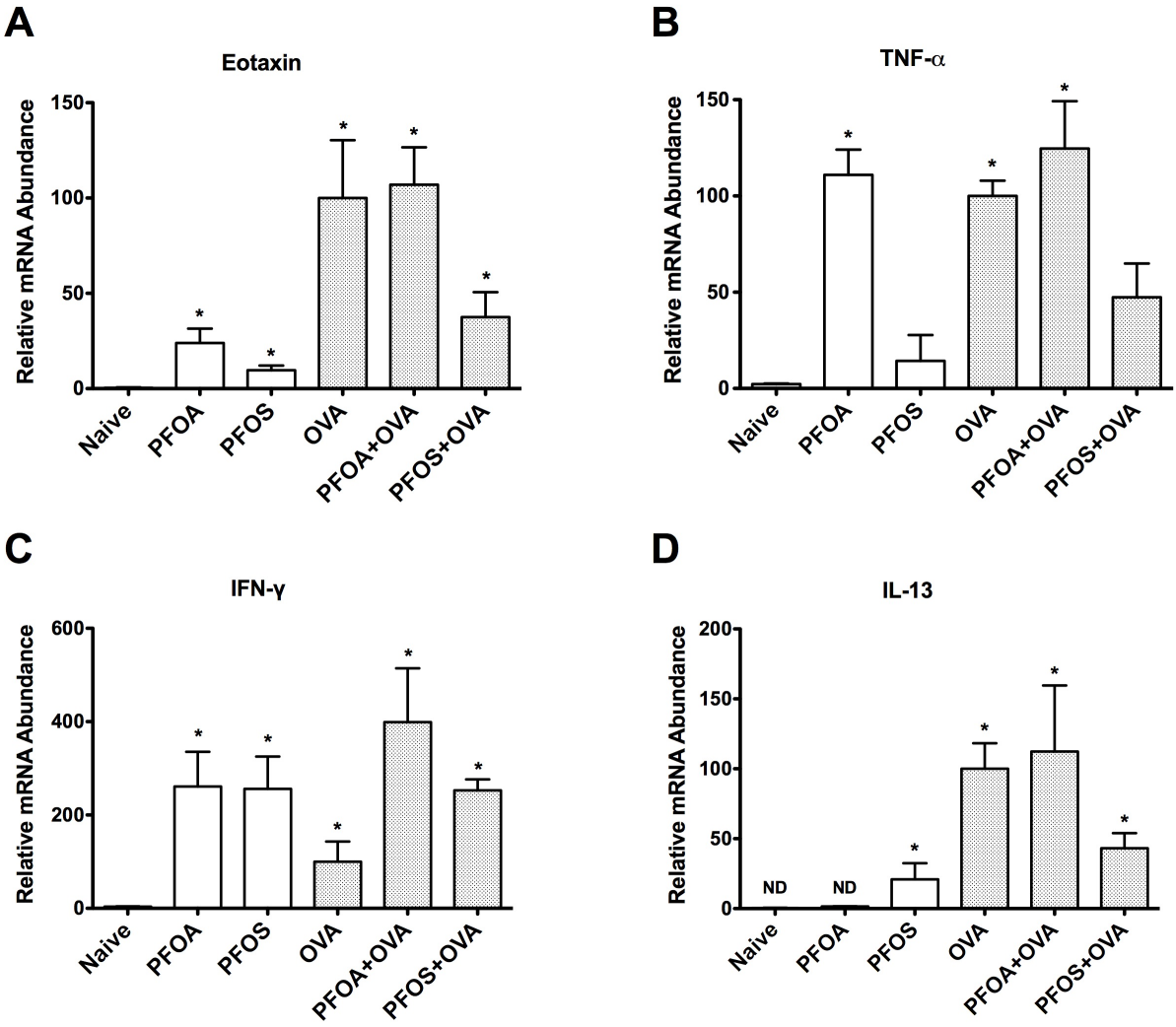

Fig 6.9. *Relative mRNA abundance of inflammatory cytokines in mouse lungs exposed to dietary PFOA and PFOS.* mRNA abundance was measured using quantitative RT-PCR, with normalization to an internal standard - ribosomal subunit 18S. Relative expression between groups was compared based on ΔΔCt values for PFOA and PFOS exposure alone **(PFOA; PFOS)**, ovalbumin sensitization and challenge **(OVA)**, or OVA sensitization and challenge in combination with PFOA or PFOS exposure **(PFOA+OVA; PFOS+OVA).** All data are plotted relative to the abundance of mRNA for each target that was detected in the OVA-only mice. IL-13 C_t value for chemical-naïve and PFOA exposed mice exceeded 35 cycles, indicating IL-13 transcript abundance was below detection limits. Significant differences from the chemical-naïve mice were determined by ANOVA and are denoted with **(*)** when $P < 0.5$. Error bars represent the standard error of mean (±SEM). Number of animals per group was three, and experimental triplicates were done for each animal. Abbreviations: **(ND)** – not detected ($C_t > 35$); TNF-α - tumor necrosis factor; IFN-γ - interferon γ; and, IL-13 - interleukin 13.

Table 6.9. Total and differential cell counts in bronchoalveolar lavage fluid collected from mice that were exposed to PFOA, FTOH or PFOS

	Naive	PFOA	FTOH	PFOS
Total cell count, $x10^4$	2.28 ± 0.17	58.1 ± 10.8†	2.31 ± 0.22	1.99 ± 0.25
Macrophage, $x10^4$	2.10 ± 0.19	56.8 ± 10.8†	2.10 ± 0.25	1.88 ± 0.25
Eosinophil, $x10^4$	0.06 ± 0.02	0.68 ±0.52	0.05 ± 0.02	0.05 ± 0.03
Neutrophil, $x10^4$	0.04 ± 0.01	0.09 ±0.08	0.10 ± 0.02	0.04 ± 0.02
Lymphocyte, $x10^4$	0.06 ± 0.03	0.56 ±0.36	0.06 ± 0.02	0.02 ± 0.01

Values are mean ± SE. **(†)** indicates significant difference compared to naïve ($P<0.05$)

Table 6.10. Total and differential cell counts in bronchoalveolar lavage fluid collected from mice that were exposed to the PFOA, FTOH or PFOS and were also sensitized and challenged with ovalbumin

	OVA-only	PFOA +OVA	FTOH +OVA	PFOS +OVA
Total cell count, $x10^4$	77.6 ± 15.0	89.0 ± 19.0	13.4 ± 4.7†	24.2 ± 3.0†
Macrophage, $x10^4$	40.1 ± 9.6	45.6 ± 6.2	6.1 ± 2.5†	14.1 ± 2.7†
Eosinophil, $x10^4$	20.2 ± 6.1	21.1 ± 9.9	3.4 ± 2.7†	3.8 ± 0.8
Neutrophil, $x10^4$	9.8 ± 2.6	15.3 ± 4.4	2.6 ± 1.5†	3.7 ± 1.4
Lymphocyte, $x10^4$	7.5 ± 2.8	7.0 ± 2.0	1.2 ± 0.7	2.6 ± 0.2

Values are mean ± SE. OVA, ovalbumin. **(†)** indicates significant difference compared to OVA-only ($P<0.05$)

Table 6.11. Semi-quantitative goblet cell and mucus score of large airways with cross-section lumen area > 1200 μm^2

	Mean score	Standard error
Naïve	0.208	0.150
PFOA	0.167	0.150
FTOH	0.167	0.150
PFOS	0.000	0.165
OVA-only	2.042†	0.150
PFOA+OVA	2.167†	0.150
FTOH+OVA	1.917†	0.150
PFOS+OVA	2.042†	0.150

Means are the average of scores from twelve conducting airways from four different animals. Goblet cell metaplasia and mucus secretion was scored from 0 to 3; 0 indicating no presence of goblet cell while 3 indicate severe goblet cell hyperplasia with greater than 2/3 of the airway epithelial stained with Periodic Acid Schiff stain. **(†)** indicates significant difference compared to the naïve ($P<0.05$).

Table 6.12. qPCR measurement of cytokine mRNA abundance in murine lungs.

	Eotaxin		TNF-α	
Treatment	$\Delta\Delta C_t$ ($x10^{-4}$)	Relative to OVA	$\Delta\Delta C_t$ ($x10^{-4}$)	Relative to OVA
Naïve	0.27 ± 0.17	0.44 ± 0.28	0.45 ± 0.07	2.26 ± 0.35
PFOA	14.54 ± 4.57*	23.9 ± 7.52	21.97 ± 2.59 *	111 ±13.1
PFOS	5.87 ± 1.57 *	9.65 ± 2.42	2.84 ± 2.65	14.4 ± 13.4
OVA	60.75 ± 18.4 *	100 ± 30.4	19.80 ± 1.57 *	100 ± 7.84
PFOA+OVA	65.0 ± 11.9 *	107 ± 19.6	24.68 ± 4.87 *	125 ± 24.6
PFOS+OVA	22.80 ± 7.95 *	37.5 ± 13.1	9.38 ± 3.46	47.4 ± 17.5
	IFN-γ		IL-13	
Treatment	$\Delta\Delta C_t$ ($x10^{-4}$)	Relative to OVA	$\Delta\Delta C_t$ ($x10^{-4}$)	Relative to OVA
Naïve	1.60 ± 0.22	3.78 ± 0.53	0.03 ± 0.01 ND	0.40 ± 0.16
PFOA	110.4 ± 31.4 *	261 ± 74.3	0.10 ± 0.00 ND	1.58 ± 0.03
PFOS	108.2 ± 29.3 *	255 ± 69.4	1.37 ± 0.75 *	20.9 ± 11.5
OVA	42.3 ± 18.3*	100 ± 43.3	6.54 ± 1.20 *	100 ± 18.3
PFOA+OVA	168.6 ± 48.8 *	399 ± 116	7.34 ± 3.09 *	112 ± 47.2
PFOS+OVA	106.8 ± 10.0 *	253 ± 23.7	2.82 ± 0.71 *	43.2 ± 10.8

Data are preseted as mean $\Delta\Delta C_t$ ± SEM. Means are average of values from three animals for each group. ANOVA followed by Bonferroni post-test was used to compare $\Delta\Delta C_t$ with the naïve and OVA-only group. **(*)** indicate significant difference compared to the naïve group, $P< 0.05$. **(†)** indicates significant difference compared to the OVA group, $P<0.05$. ND (not detected) indicates $C_t > 35$, which is considered outside detectable experimental threshold.

Table 6.13. The variance of ELISA performed on whole lung lysates

		TNF-a (pg/mL)	**IL-5 (pg/mL)**	**IFN-g (pg/mL)**
Naïve (N=3)	Average	5.20	13.32	31.81
	Variance	1.78	113.78	442.12
OVA (N= 7)	Average	4.78	11.07	32.14
	Variance	0.64	8.74	137.31
PFOA (N=7)	Average	4.93	11.77	36.96
	Variance	0.41	44.89	100.50
PFOA+OVA(N=6)	Average	5.13	17.76	35.18
	Variance	1.59	47.89	134.05
PFOS (N=3)	Average	3.14	8.35	24.51
	Variance	1.55	12.72	45.83
PFOS+OVA (N=3)	Average	3.91	12.52	31.04
	Variance	2.16	22.50	76.26
FTOH (N=7)	Average	3.12	11.86	35.12
	Variance	1.00	29.15	148.81
FTOH+OVA (N=3)	Average	4.16	8.87	14.63
	Variance	0.89	14.20	13.47

Data are presented with mean (pg/mL) and variance for each group. Cytokine level was measured from each biological sample in duplicates.

7. DISCUSSION

Here we evaluated and demonstrated in mice that *in-utero*-through-postnatal exposure to PFOA on its own led to exposed offspring acquiring AHR. To our knowledge, such impact on lung function has not been reported elsewhere. Moreover, this study was the first of its kind to demonstrate the impact of PFCs on lung function by utilizing a unique chronic PFCs exposure protocol, beginning *in utero* by exposing pregnant dams and then continuing throughout early infancy and adolescence of the offspring by exposing nursing dams and weaned pups to PFOA, FTOH or PFOS. This approach resulted in PFC exposure that spanned all critical stages of development, thus mimicking human exposure in the global environment. Therefore, our study offers a unique platform to gauge the potential adverse effects of early life and continued exposure to PFCs.

Prior to our study, dermal exposure of mice to high doses of PFOA had been demonstrated to augment ovalbumin (OVA) induced IgE response and airway hyperreactivity, and *in utero* exposure to PFOA and PFOS caused significant histological and morphometric changes in the newborns (51,52,70). Our findings provide new evidence that the impact of PFCs on developing lungs can ultimately lead to functional changes later in life. Furthermore, our finding provides support to a recent epidemiological study that links PFC exposures to juvenile asthma (45), and supports the currently held public opinion that minimization of exposure to PFCs is in the best interest of children and expectant mothers.

One of the intriguing findings of this study was that, despite similarities in structure and function of PFOA and PFOS as PPARα and β agonists, the effects of long-term exposure to each compound on airway inflammation and lung function have several distinct features. PFOA exposure alone, but not PFOS alone, was associated with significant airway

hyperresponsiveness. PFOA exposure was linked to increased numbers of lung macrophages, whereas PFOS had no such effect. However, exposure to any of PFOA, FTOH or PFOS was associated with elevated expression of the immune regulator, IFN-γ in the lungs. This implies tat the elevation of IFN-γ is no sufficient to produce all of the effects observed by some PFCs. Indeed, PFOS ingestion was associated with suppressed OVA-induced leukocyte infiltration to the lungs, while PFOA ingestion had no detectable impact. Suppression of airway inflammation by PFOS is consistent with evidence that PFOS and PFOA can have immunosuppressive capacity (71-73).

This is intriguing because macrophages engulf inhaled inert particles and initiate an inflammatory response by releasing inflammatory cytokines (such as TNF-α and IFN-γ) and neutrophil chemoattractants (KC), all of which have been implicated in airway inflammation and hyperresponsiveness (74,75). Indeed, mRNA abundances of TNFα and IFN-γ were elevated in PFOA exposed mice (Fig. 6.9), implicating a change in the local immune response that may have contributed to PFC induced AHR. The level of IFN-γ mRNA was elevated in all three exposure groups (Fig. 6.9) and this effect was retained in mice that were also challenged with OVA. This is interesting because the accumulation of macrophages in several disorders (for example, in adipose tissue at sites of atherosclerotic plaque formation) is associated with local inflammation that includes IFN-γ production as part of the interactions among resident and infiltrating immune cells with macrophages in a local immune network (76,77). IFN-γ modulates innate and adaptive immunity against, viral, intracellular bacterial infections and an allergic insult, and it is an important activator of macrophages (77). Though our study was not designed to delineate the mechanisms that link PFC exposure to increased IFN-γ expression, our findings do support future work in this area. Moreover, our work uncovers areas for further investigation,

and suggests that examination of the impact of chronic PFC exposure on the response to infectious agents, and the resulting changes in lung inflammation and function, should be of interest.

In light of the increase in macrophage presence only seen with PFOA exposure, the altered inflammatory response to OVA by FTOH and PFOS is surprising. These PFCs is known to modulate immune function by acting as agonists for the peroxisome proliferator-activated receptors (PPAR) α, β and γ (55). PPARs are widely expressed in diverse cell types including immune and pulmonary structural cells and can act as a regulator of gene transcription through binding to specific response elements or peroxisome proliferator response elements (PPREs). PPARγ, in particular, regulates energy metabolism, cell differentiation, apoptosis and inflammation (56). Activated PPARγ stimulates the differentiation of monocytes to macrophages, and inhibits the induction of inducible nitric oxide synthase, metallanoproteinase-9 and scavenger receptor A transcription (58). PPARγ activation inhibits the expression of monocyte-chemoattractant protein-1, vascular cell adhesion molecule-1 and intracellular adhesion molecule; thus PPARγ activation interferes with chemo-attraction and cell adhesion of monocytes, and T- lymphocytes (57). Moreover, PPARγ also acts as a trans-repressor of macrophage inflammatory genes (59).

Aside from their role as PPARγ agonists, both PFOA and PFOS modulate the immune response by acting as PPARα agonists (70). PPARα agonists, such as gemfibrozil, ciprofibrate, and fenofibrate, have been demonstrated to increase the production of IL-4 in human T-cell lines and cause a shift in cytokine levels by inhibiting interferon-gamma (IFN-γ) (61). In line with those effects, PFOA is thought to augment the Th2 response and subsequently increase airway hyperreactivity through its action on PPARα. Indeed, both PFOA and PFOS show greater

affinity for and activation of PPARα than PPARγ does, suggesting that the main target for PFOA and PFOS is PPARα (55).

All together, the distinctive impact of the two compounds on the lungs likely arises from differential affinity and activation of PPAR by PFOA and PFOS. PFOS has a higher affinity for PPARγ than PFOA, and PFOA has a higher affinity for, and greater activation of PPARα than PFOS does (55). In this regard, future studies using a murine PPAR knockout model will be important in elucidating the mechanism of AHR observed in this study.

It will also be meaningful to investigate the impact of PFCs on macrophage subtypes and phenotype because proliferation of one subtype (M1 or M2) has been implicated in infectious disease; and polarization of macrophages often has functional consequences for local tissue immunity (78). Future studies should also focus on tissue-resident macrophages that have prenatal origins within the lungs, because early life insults to these cells may underpin the lung dysfunction associated with PFOA, FTOH and PFOS exposure. Alveolar macrophages will be a good candidates to study because they have prenatal origins in the lungs, act as immune surveillance for inhaled pathogens, and regulate clearance of surfactant (79-81).

Another surprising finding of this study is that despite the impact of FTOH and PFOS on airway inflammation, none of the compounds tested impacted the magnitude of OVA-induced AHR. Indeed, this is in disagreement with findings from an acute dermal PFOA exposure protocol that showed enhanced airway hyperreactivity in mice exposed to PFOA and OVA (70). At first glance, the difference may be attributed to differences in PFC dosage: the dermal study utilized 2.5 mg PFOA/kg body weight/day and our protocol utilized ~1 mg PFOA/kg body weight/day. However, our protocol includes maternal exposure during gestation and nursing (42 days at 1 mg/kg) as well as 9 weeks (63 days at 1 mg/kg) of PFOA or PFOS

ingestion post-weaning. In total, this study delivered a cumulative exposure dose of approximately 105 mg/kg (42 days +63 days at 1 mg/kg). In contrast, the acute dermal exposure study delivered 2.5 mg/kg for 4 days, for a cumulative dose of only 10 mg/kg. Hence, the lack of impact on lung function would not appear to be linked to any deficit in the magnitude of PFC exposure.

Of note, the dermal study utilized whole body plethysmography instead of the force oscillation method utilized in this study. Whole body plethysmography provides nonspecific respiratory mechanics, while the force oscillation method provides a more specific measures of conducting airways mechanics (67). Therefore, enhanced OVA-induced airway hyperreactivity with higher-dose PFOA and measured by plethysmography could reflect more global changes in lung physiology, whereas the lack of effect on Rn measured by force oscillation likely is more reflective of the airway response.

One may argue that the conclusion of this experimental finding, however, should be taken with caution because the dose range used for OVA sensitization and challenge presented here was sufficient to reach maximum detectable changes in lung, thereby precluding any potential additive impact that PFCs could have. However, this possibility is unlikely because the Rn values that were measured across groups were as high as 2.60 cmH2O·s/mL, with the mean Rn in the OVA-only group being only 1.97 cmH2O·s/mL. This suggests murine airways are capable of generating greater airflow limitation than what was measured in the OVA-only group. Hence, it is unlikely that any real augmentation of Rn by PFC exposure remained undetected due to the technical limitations of using a high concentration of OVA or limits in the measurement range of the small animal ventilator. Nevertheless, in future studies, submaximal allergen sensitization may be used to reveal any additive capacity of xenobiotics to enhance OVA-

induced AHR. To date, Midoro-Horiuti *et al.* were successful in using such a submaximal OVA model to show that Bisphenol A exposure enhanced OVA-induced airway hyperreactivity (2).

In addition, our protocol was to assess AHR at 48 hrs post allergen challenge, when AHR was at its peak in OVA-only animals. This time point may not be ideal for tracking peak cytokine expression in lung tissue, since cytokine levels most likely reach peak values before maximum AHR is attained. Therefore, our cytokine mRNA data may not necessarily reflect causal mechanisms. Indeed, the cytokine mRNA level measured was relatively low at this time point, being in the order of <1% of ribosomal 18s. Future studies to assess the impact of PFC exposure on cytokine expression as a causal relationship (i.e., immune suppression) should make use of earlier time points.

Even in the absence of any exacerbation of OVA-induced AHR by PFCs, it is notable and potentially alarming that PFOA or FTOH alone induced AHR in mice. The magnitude of PFOA and FTOH-induced AHR was comparable to that of OVA-induced AHR. This finding is striking because adult dams showed no change in their respiratory mechanics in spite of receiving the same dietary PFOA for six weeks during pregnancy and lactation (82). This suggests that exposure to PFCs specifically in early development (fetal and postnatal) is necessary for the development of PFC-induced AHR. Of course, the experimental design did not exclude the possibility that exposure to PFOA or PFOS *in utero* only, during early infancy only, or in early adulthood only may be enough to have an impact on the susceptibility to develop an asthma phenotype. Nevertheless, our model most resembles typical human environmental exposure that span over long period of accumulative exposure and therefore merits consideration.

Besides these key findings, a few interesting observations were made that are worthy of note. First is the association of liver enlargement with ingested PFOA and PFOS. This

association was not surprising at first given that many previous studies have demonstrated such an effect in PFOA and PFOS exposed mice (49,50). Interestingly, however, mice that inhaled FTOH did not show liver enlargement, despite show a serum PFOA level similar to mice that ingested PFOA (see Fig. 6.1 & 6.2). This was surprising because a previous study where FTOH was administered orally also showed liver enlargement (83). Our finding implies that liver enlargement is a consequence specific to dietary (oral) exposure to these xenobiotics.

A second observation of note is that PFOA exposure, at a dose of 1mg/kg body weight/day, resulted in a serum PFOA concentration of 4800 ± 1100 ng/mL or 4.8 ± 1.1 mg/L, almost one order of magnitude higher than serum levels reported in occupationally exposed persons (422-999 ng/mL) or that reported for individuals living in areas of high environmental exposure (155-556 ng/mL) (37). A more recent study measured considerably higher human serum levels: the serum PFOA concentration measured in retired fluorochemical production workers ranged from 72 ng/mL to 5100 ng/mL in 26 individuals (33). Moreover, the detected level of circulating PFOA in our murine model is two to three orders of magnitude higher than the 0.5-20 ng/mL detected in the general public (31, 38). Previous animal studies have utilized a much higher dose than we chose (50-52,70). Toxicological findings of animal studies using higher doses should be approached with caution when extrapolating animal model findings to humans, especially with developmental models. Nevertheless, our model most probably mimics the exposure level of the highly exposed occupational workers and individuals living in area of high environmental exposures (except these workers were not exposed in utero or as children, unless some of them were pregnant while working). This warrants an additional study with PFOA concentration one or two orders of magnitude lower than 4 mg PFOA/ kg feed/day (or 1 mg/ kg body weight/ day) to bring the model closer to exposures level in general population.

8. CONCLUSION

In conclusion, we demonstrated in this study that in allergen-naïve mice, *in utero*-through-adulthood exposure to PFOA alone was sufficient to induce lung inflammation (characterized by macrophage accumulation and IFN-γ expression) as well as AHR, a hallmark symptom of asthma (13). A similar increase in IFN-γ expression as well as AHR was seen in mice exposed to FTOH. Chronic exposure of mice to PFOS increased airway sensitivity to a bronchoconstrictor, agonist, along with the suppression of allergic airway inflammation. These findings add to the awareness of the toxicity of these compounds. In the past, increased awareness of the potential toxicity of PFOS to humans and wildlife resulted in a voluntary phase-out in production by manufacturing companies more than a decade ago, and this has resulted in a decline in serum PFOS concentration in the general public (83). Moreover, our findings are important because they strongly support the current production phase-out of PFOA by eight major manufacturers, through a voluntary stewardship agreement with United States Environmental Protection Agency to eliminate global PFOA production by 2015 (85). Our study also highlights the importance of continued monitoring of these chemicals not only because these chemicals persist in the environment and in the human population, but also because they may impact developing children (31,33). Finally, taken into consideration with epidemiological studies that link PFOA exposure to juvenile asthma, our findings support the currently held public opinion that minimization of exposure to PFCs is in the best interest of children and expectant mothers.

9. References

1. **United States Food and Drug Administration**. Bisphenol A (BPA): Use in food contact application [Internet]. http://www.fda.gov/newsevents/publichealthfocus/ucm064437.htm [cited 2014 Oct 15].

2. **Midoro-Horiuti T, Tiwari R, Watson CS, Goldblum RM.** Maternal Bisphenol A exposure promotes the development of experimental asthma in mouse pups. *Environ Health Perspect* 2009; 118(2):273–7.

3. **Van Winkle LS, Murphy SR, Boetticher MV, VandeVoort CA.** Fetal exposure of Rhesus Macaques to Bisphenol A alters cellular development of the conducting airway by changing epithelial secretory product expression. *Environ Health Perspect* 2013; 121(8):912–8.

4. **Bousquet J, Clark TJH, Hurd S, Khaltaev N, Lenfant C, O'Byrne P, et al.** GINA guidelines on asthma and beyond. *Allergy* 2007;62(2).

5. **Statistic Canada.** Health indicator profile, annual estimates, by age group and sex, Canada, provinces, territories, health regions (2012 boundaries) and peer groups. CANSIM (database). (accessed online January 21, 2014)

6. **Bahadori K, Doyle-Waters MM, Marra C, Lynd L, Alasaly K, Swiston J, et al.** Economic burden of asthma: a systematic review. *BMC Pulm Med* 2009; 9:24.

7. **Masoli M, Fabian D, Holt S, Beasley R.** The global burden of asthma: executive summary of the GINA Dissemination Committee report. *Allergy* 2004; 59(5):469–78.

8. **Poon AH, Eidelman DH, Martin JG, Laprise C, Hamid Q.** Pathogenesis of severe asthma. *Clin Exp Allergy* 2012; 42(5):625–37.

9. **Iwamoto I, Nakajima H, Endo H, Yoshida S.** Interferon gamma regulates antigen-induced eosinophil recruitment into the mouse airways by inhibiting the infiltration of CD4+ T cells. *J Exp Med* 1993;177(2):573–6.

10. **Nakajima H, Takatsu K.** Role of cytokines in allergic airway inflammation. *Int Arch Allery Immunol* 2007; 142(4):265–73.

11. **Grünig G, Warnock M, Wakil AE, Venkayya R, Brombacher F, Rennick DM, et al.** Requirement for IL-13 independently of IL-4 in experimental asthma. *Science* 1998; 282(5397): 2261–3.

12. **Walter DM, McIntire JJ, Berry G, McKenzie AN, Donaldson DD, DeKruyff RH, et al.** Critical role for IL-13 in the development of allergen-induced airway hyperreactivity. *J Immunol* 2001;167(8):4668–75.

13. **Postma DS, Kerstjens H.** Characteristics of airway hyperresponsiveness in asthma and chronic obstructive pulmonary disease. *Am J Respir Crit Care Med* 1998;158(Supplement 2):S187–92.

14. **Cockroft D, Davis B.** Mechanisms of airway hyperresponsiveness. *J Allergy Clin Immun* 2006; 118(3):551–9.

15. **Wills-Karp M, Luyimbazi J, Xu X, Schofield B, al E.** Interleukin-13: central mediator of allergic asthma. *Science* 1998; 282: 2258–61.

16. **Pichavant M, Goya S, Meyer EH, Johnston RA, Kim HY,** Matangkasombut P, et al. Ozone exposure in a mouse model induces airway hyperreactivity that requires the presence of natural killer T cells and IL-17. *J Exp Med* 2008; 205(2):385–93.

17. **Ohta K, Yamashita N, Tajima M, Miyasaka T, Nakano J, Nakajima M, et al.** Diesel exhaust particulate induces airway hyperresponsiveness in a murine model: Essential role of GM-CSF. *J Allergy Clin Immun* 1999 Nov;104(5):1024–30.

18. **Simpson A, Maniatis N, Jury F, et al.** Polymorphisms in a disintegrin and metalloprotease 33 (ADAM33) predict impaired early-life lung function. *Am J Respir Crit Care Med* 2005; 172:55-60.

19. **Jedrychowski W, Galas A, Pac A, Flak E, Camman D, Rauh V, et al.** Prenatal ambient air exposure to polycyclic aromatic hydrocarbons and the occurrence of respiratory symptoms over the first year of life. *Eur J Epidemiol* 2005; 20(9):775–82.

20. **Gilliland FD, Li YF, Peters JM.** Effects of maternal smoking during pregnancy and environmental tobacco smoke on asthma and wheezing in children. *Am J Respir Crit Care Med* 2001; 163:429–36.

21. **Xu B, Pekkanen J, Järvelin MR, Olsen P, al E.** Maternal infections in pregnancy and the development of asthma among offspring. *J Epidemiol* 1999; 28:723–27.

22. **Prescott SL.** Maternal allergen exposure as a risk factor for childhood asthma. *Curr Allergy Asthma Rep* 2006; 6(1):75–80.

23. **Auten RL, Potts EN, Mason SN, Fischer B, Huang Y, Foster WM.** Maternal exposure to particulate matter increases postnatal ozone-induced airway hyperreactivity in juvenile mice. *Am J Respir Crit Care Med* 2009; 180(12):1218–26.

24. **Fedulov AV, Leme A, Yang Z, Dahl M, Lim R, Mariani TJ, et al.** Pulmonary exposure to particles during pregnancy causes increased neonatal asthma susceptibility. *Am J Resp Cell Mol* 2008; 38(1):57–67.

25. **Shoeib M, Harner T, M Webster G, Lee SC.** Indoor sources of poly- and perfluorinated compounds (PFCS) in Vancouver, Canada: Implications for human exposure. *Environ Sci Technol* 2011; 45(19):7999–8005.

26. **Haug LS, Huber S, Schlabach M, Becher G, Thomsen C.** Investigation on per- and polyfluorinated compounds in paired samples of house dust and indoor air from Norwegian homes. *Environ Sci Technol* 2011; 45(19):7991–8.

27. **Stock NL, Lau FK, Ellis DA, Martin JW, Muir DCG, Mabury SA.** Polyfluorinated telomer alcohols and sulfonamides in the North American troposphere. *Environ Sci Technol* 2004; 38(4):991–6.

28. **Llorca M, Farré M, Picó Y, Müller J, Knepper TP, Barceló D.** Analysis of Perfluoroalkyl substances in waters from Germany and Spain. *Sci Total Environ* 2012; 431; 139–50.

29. **Butt CM, Berger U, Bossi R, Tomy GT.** Levels and trends of poly-and perfluorinated compounds in the arctic environment. *Sci Total Environ* 2010; 408(15):2936–65.

30. **Zhang T, Wu Q, Sun HW, Zhang XZ, Yun SH, Kannan K.** Perfluorinated compounds in whole blood samples from infants, children, and adults in China. *Environ Sci Technol* 2010; 44(11):4341–7.

31. **Olsen GW, Lange CC, Ellefson ME, Mair DC, Church TR, Goldberg CL, et al**. Temporal trends of perfluoroalkyl concentrations in American Red Cross adult blood donors, 2000–2010. *Environ Sci Technol* 2012; 46(11):6330–8.

32. **Kim S, Choi K, Ji K, Seo J, Kho Y, Park J, et al.** Trans-placental transfer of thirteen perfluorinated compounds and relations with fetal thyroid hormones. *Environ Sci Technol* 2011; 45(17):7465–72.

33. **Olsen GW, Burris JM, Ehresman DJ, Froehlich JW, Seacat AM, Butenhoff JL, et al.** Half-life of serum elimination of perfluorooctanesulfonate, perfluorohexanesulfonate, and perfluorooctanoate in retired fluorochemical production workers. *Environ Health Perspect* 2007; 115(9):1298–305.

34. **Yeung LWY, So MK, Jiang G, Taniyasu S, Yamashita N, Song M, et al.** Perfluorooctanesulfonate and related fluorochemicals in human blood samples from China. *Environ Sci Technol* 2006; 40(3):715–20.

35. **Kärrman A, Mueller JF, van Bavel B, Harden F, Toms L-ML, Lindström G.** Levels of 12 perfluorinated chemicals in pooled australian serum, collected 2002−2003, in relation to age, gender, and region. *Environ Sci Technol* 2006; 40(12):3742–8.

36. **Kannan K, Corsolini S, Falandysz J, Fillmann G, Kumar KS, Loganathan BG, et al.** Perfluorooctanesulfonate and related fluorochemicals in human blood from several countries. *Environ Sci Technol* 2004; 38(17):4489–95.

37. **Emmett EA, Shofer FS, Zhang H, Freeman D, Desai C, Shaw LM.** Community exposure to perfluorooctanoate: relationships between serum concentrations and exposure sources. *J Occup Environ Med* 2006; 48(8):759–70.

38. **Lau C, Anitole K, Hodes C, Lai D, Pfahles-Hutchens A, Seed J.** Perfluoroalkyl scids: A teview of monitoring and toxicological findings. *Toxicol Sci* 2007; 99(2):366–94.

39. **Tittlemier SA, Pepper K, Seymour C, Moisey J, Bronson R, Cao X-L, et al.** Dietary exposure of Canadians to perfluorinated carboxylates and perfluorooctane sulfonate via consumption of meat, fish, fast foods, and food items prepared in their packaging. *J Agric Food Chem* 2007; 55(8):3203–10.

40. **Stahl T, Mattern D, Brunn H.** Toxicology of perfluorinated compounds. Environ Sci Eur 2011; 23:38.

41. **Alexander BH, Olsen GW.** Bladder cancer in perfluorooctanesulfonyl fluoride manufacturing workers. *Ann Epidemiol* 2007; 17(6):471–8.

42. **Eriksen KT, Raaschou-Nielsen O, Sørensen M, Roursgaard M, Loft S, Møller P.** Genotoxic potential of the perfluorinated chemicals PFOA, PFOS, PFBS, PFNA and PFHxA in human HepG2 cells. *Mutat Res* 2010; 700(1-2):39–43.

43. **Alexander BH, Olsen GW, Burris JM, Mandel JH, Mandel JS.** Mortality of employees of a perfluorooctanesulphonyl fluoride manufacturing facility. Occup Environ Med 2003; 60: 722–29.

44. **Fei C, McLaughlin JK, Tarone RE, Olsen J**. Perfluorinated chemicals and fetal growth: A study within the Danish national birth cohort. *Environ Health Persp* 2007; 115(11):1677–82.

45. **Dong G-H, Tung K-Y, Tsai C-H, Liu M-M, Wang D, Liu W, et al.** Serum polyfluoroalkyl concentrations, asthma outcomes, and immunological markers in a case-control study of Taiwanese children. *Environ Health Persp* 2013; 121: 507–13.

46. **Anderson-Mahoney P, Kotlerman J, Takhar H, Gray D, Dahlgren J.** Self-reported health effects among community residents exposed to perfluorooctanoate. *J Environ Occup Health Policy* 2008; 18(2):129–43.

47. **Monroy R, Morrison K, Teo K, Atkinson S, Kubwabo C, Stewart B, et al.** Serum levels of perfluoroalkyl compounds in human maternal and umbilical cord blood samples. *Environ Res* 2008; 108(1):56–62.

48. **Lau C, Butenhoff JL, Rogers JM.** The developmental toxicity of perfluoroalkyl acids and their derivatives. *Toxicol Appl Pharmacol*; 198(2):231–41.

49. **Lau C, Thibodeaux JR, Hanson RG, Rogers JM, Grey BE, Stanton ME, et al.** Exposure to perfluorooctane sulfonate during pregnancy in rat and mouse. *Toxicol Sci* 2003; 74(2):382–92.

50. **Lau C, Thibodeaux JR, Hanson RG, Narotsky MG, Rogers JM, Lindstrom AB, et al.** Effects of perfluorooctanoic acid exposure during pregnancy in the mouse. *Toxicol Sci* 2006; 90(2):510–8.

51. **Grasty RC, Grey BE, Lau CS, Rogers JM.** Prenatal window of susceptibility to perfluorooctane sulfonate-induced neonatal mortality in the Sprague-Dawley rat. *Birth Defect Res B* 2003; 68(6):465–71.

52. **Grasty RC, Bjork JA, Wallace KB, Lau CS, Rogers JM.** Effects of prenatal perfluorooctane sulfonate (PFOS) exposure on lung maturation in the perinatal rat. *Birth Defect Res B* 2005; 74(5):405–16.

53. **Lehmler HJ, Xie W, Bothun GD, Bummer PM, Knutson BL.** Mixing of perfluorooctanesulfonic acid (PFOS) potassium salt with dipalmitoyl phosphatidylcholine (DPPC). *Colloids Surface B* 2006; 51(1):25–9.

54. **Gordon SC, Schurch S, Amrein M, Schoel M.** Effects of perrfluorinated acids on pulmonary surfactant properties in vitro. *Toxicologist* 2007; 96:91.

55. **Heuvel JPV, Thompson JT, Frame SR, Gillies PJ.** Differential activation of nuclear receptors by perfluorinated fatty acid analogs and natural fatty acids: A comparison of human, nouse, and rat peroxisome proliferator-activated receptor- α, - β, and - γ, Liver X Receptor- β, and Retinoid X Receptor. *Toxicol Sci* 2006; 92(2):476–89.

56. **Houseknecht KL, Cole BM, Steele PJ.** Peroxisome proliferator-activated receptor gamma (PPARγ) and its ligands: a review. *Domest Anim Endocrin* 2002; 22(1):1–23.

57. **Debril M-B, Renaud J-P, Fajas L, Auwerx J.** The pleiotropic functions of peroxisome proliferator-activated receptor γ. J Mol Med 2001; 79(1):30–47.

58. **Ricote M, Li AC, Willson TM, Kelly CJ, Glass CK.** The peroxisome proliferator-activated receptor-gamma is a negative regulator of macrophage activation. *Nature* 1998; 391(6662):79–82.

59. **Pascual G, Fong AL, Ogawa S, Gamliel A, Li AC, Perissi V, et al.** A SUMOylation-dependent pathway mediates transrepression of inflammatory response genes by PPAR-γ. *Nature* 2005; 437(7059):759–63.

60. **Trifilieff A, Bench A, Hanley M, Bayley D, Campbell E, Whittaker P.** PPAR- αand - γ but not - δ agonists inhibit airway inflammation in a murine model of asthma: in vitro evidence for an NF-κB-independent effect. Brit J Pharmacol 2003; 139(1):163–71.

61. **Lovett-Racke AE, Hussain RZ, Northrop S, Choy J, Rocchini A, Matthes L, et al.** Peroxisome proliferator-activated receptor alpha agonists as therapy for autoimmune disease. *J Immunol* 2004; 172(9):5790–8.

62. **Singh TSK, Lee S, Kim H-H, Choi JK, Kim S-H.** Perfluorooctanoic acid induces mast cell-mediated allergic inflammation by the release of histamine and inflammatory mediators. *Toxicol Lett* 2012; 210(1):64–70.

63. **Ryu MH, Jha A, Ojo OO, Mahood TH, Basu S, Detillieux KA, Nikoobakht N, Wong CS, Loewen M, Becker AB, Halayko AJ**. Chronic exposure to perfluorinated compounds: Impact on airway hyperresponsiveness and inflammation. *Am J Physiol - Lung Cell Mol Physiol* 2014; 307(10):L765-774.

64. **Mosch C, Kiranoglu M, Fromme H, Völkel W.** Simultaneous quantitation of perfluoroalkyl acids in human serum and breast milk using on-line sample preparation by HPLC column switching coupled to ESI-MS/MS. *J Chromatogr B* 2010; 878(27):2652–8.

65. **Chan E, Burstyn I, Cherry N, Bamforth F, Martin JW.** Perfluorinated acids and hypothyroxinemia in pregnant women. *Environ Res* 2011; 111(4):559–64.

66. **Tomioka S, Bates J, Irvin CG.** Airway and tissue mechanics in a murine model of asthma: alveolar capsule vs. forced oscillations. *J App Physiol* 2002; 93: 263–70.

67. **Irvin CG, Bates JH.** Measuring the lung function in the mouse: the challenge of size. *Respir Res* 2003; 4(1):4.

68. **Arai N, Kondo M, Izumo T, Tamaoki J, Nagai A.** Inhibition of neutrophil elastase-induced goblet cell metaplasia by tiotropium in mice. *Eur Respir J* 2010; 35(5):1164–71.

69. **Livak KJ, Schmittgen TD.** Analysis of relative gene expression data using real-time quantitative PCR and the $2 - \Delta\Delta CT$ method. *Methods* 2001;25(4):402–8.

70. **Fairley KJ, Purdy R, Kearns S, Anderson SE, Meade B.** Exposure to the immunosuppresant, perfluorooctanoic acid, enhances the murine IgE and airway hyperreactivity response to

ovalbumin. *Toxicol Sci* 2007; 97(2):375–83.

71. **DeWitt JC, Shnyra A, Badr MZ, Loveless SE, Hoban D, Frame SR, et al.** Immunotoxicity of perfluorooctanoic acid and perfluorooctane sulfonate and the role of peroxisome proliferator-activated receptor alpha. *Crit Rev Toxicol* 2009; 39: 76–94.

72. **Zheng L, Dong GH, Jin YH, He QC.** Immunotoxic changes associated with a 7-day oral exposure to perfluorooctanesulfonate (PFOS) in adult male C57BL/6 mice. *Arch Toxicol* 2009; 83:679–89.

73. **Brieger A, Bienefeld N, Hasan R, Goerlich R, Haase H.** Impact of perfluorooctanesulfonate and perfluorooctanoic acid on human peripheral leukocytes. *Toxicol In Vitro* 2011; 25(4):960–8.

74. **Thomas PS, Yates DH, Barnes PJ.** Tumor necrosis factor-alpha increases airway responsiveness and sputum neutrophilia in normal human subjects. *Am J Respir Crit Care Med* 1995; 152: 76–80.

75. **Kobzik L, Huang S, Paulauskis JD, Godleski JJ.** Particle opsonization and lung macrophage cytokine response. In vitro and in vivo analysis. *J Immunol* 1993; 151(5):2753–9.

76. **Rocha VZ, Folco EJ, Sukhova G, Shimizu K, Gotsman I, Vernon AH, et al.** Interferon- γ, a Th1 Cytokine, Regulates Fat Inflammation: A Role for Adaptive Immunity in Obesity. *Circ Res* 2008; 103(5):467–76.

77. **Yan Z-Q, Hansson GK.** Innate immunity, macrophage activation, and atherosclerosis. *Immunol Rev* 2007; 219(1):187–203.

78. **Benoit M, Desnues B, Mege JL.** Macrophage polarization in bacterial infections. J Immunol 2008; 181:3773–39.

79. **Maus UA, Koay MA, Delbeck T, Mack M, Ermert M, Ermert L, et al.** Role of resident alveolar macrophages in leukocyte traffic into the alveolar air space of intact mice. *Am J Physiol Lung Cell Mol Physiol* 2002; 282(6):L1245–52.

80. **Gautier EL, Chow A, Spanbroek R, Marcelin G, Greter M, Jakubzick C, et al.** Systemic Analysis of PPAR in mouse macrophage populations reveals marked diversity in expression with critical roles in resolution of inflammation and airway immunity. *J Immunol* 2012; 189(5):2614–24.

81. **Yona S, Kim K-W, Wolf Y, Mildner A, Varol D, Breker M, et al.** Fate mapping reveals origins and dynamics of monocytes and tissue macrophages under homeostasis. *Immunity* 2013; 38(1):79–91.

82. **Loewen M, Basu S, Halayko AJ, HayGlass K, al E.** The role of perfluooctanoic acid (PFOA) in airway hyperrepsoniveness. *Allergy, Asthma & Clinical Immunology* 2010; 6(Suppl 3): P21.

83. **Kudo N.** Induction of hepatic peroxisome proliferation by 8-2 telomer alcohol feeding in mice: formation of perfluorooctanoic acid in the liver. *Toxicol Sci 2005*; 86(2):231–8.

84. **Olsen GW, Mair DC, Church TR, Ellefson ME, Reagen WK, Boyd TM, et al.** Decline in perfluorooctanesulfonate and other polyfluoroalkyl chemicals in american red cross adult blood donors, 2000−2006. *Environ Sci Technol* 2008; 42(13):4989–95.

85. **US Environmental Protection Agency.** *2010/2015 PFOA Stewardship Program* [Online]. Unitied States Environmental Protection Agency. http://www.epa.gov/opptintr/pfoa/pups/stewardship/index.html [cited 2014 Jan 21].

86. **McConkey, CE.** Per- and Polyfluorinated Compounds in Blood and their Impact on Respiratory Problems in Young Children in Winnipeg, Manitoba. MSc Thesis. The University of Mantioba (2013). MS26241.